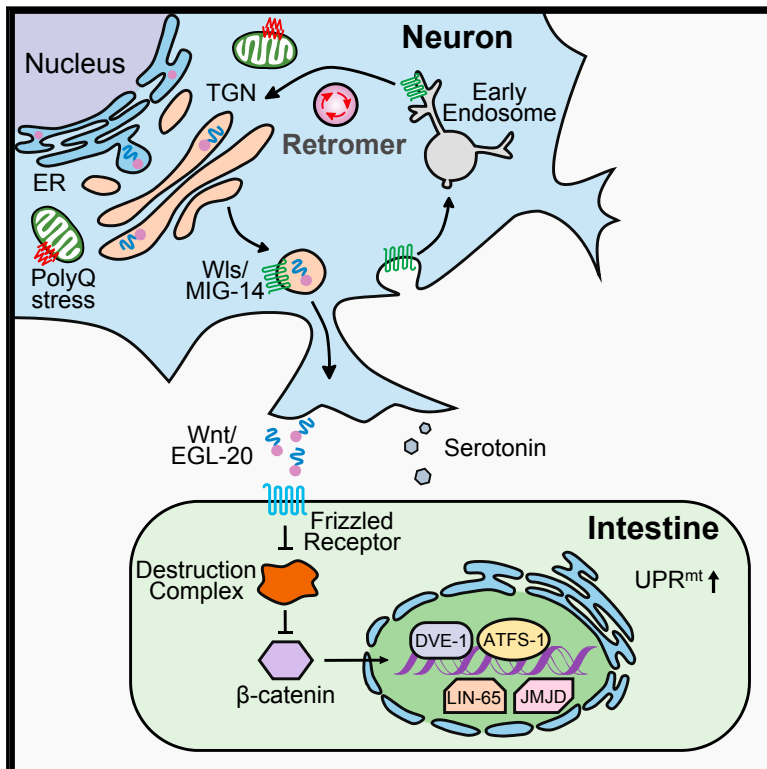


The Mitochondrial Unfolded Protein Response Is Mediated Cell-Non-autonomously by Retromer-Dependent Wnt Signaling

Graphical Abstract



Authors

Qian Zhang, Xueying Wu, Peng Chen, Limeng Liu, Nan Xin, Ye Tian, Andrew Dillin

Correspondence

ytian@genetics.ac.cn (Y.T.),
dillin@berkeley.edu (A.D.)

In Brief

The Wnt/EGL-20 relays mitochondrial stress signals from neurons to peripheral tissues.

Highlights

- The retromer complex is required for the induction of cell-non-autonomous UPR^{mt}
- Retromer retrieval of the Wntless/MIG-14 is essential for the induction of UPR^{mt}
- The Wnt/EGL-20 is essential, specific, and sufficient for the induction of UPR^{mt}
- Neuronal EGL-20-induced cell-non-autonomous UPR^{mt} requires serotonin

The Mitochondrial Unfolded Protein Response Is Mediated Cell-Non-autonomously by Retromer-Dependent Wnt Signaling

Qian Zhang,^{1,2,5} Xueying Wu,^{1,5} Peng Chen,^{1,2,5} Limeng Liu,¹ Nan Xin,⁴ Ye Tian,^{1,2,3,*} and Andrew Dillin^{4,6,*}

¹State Key Laboratory of Molecular Developmental Biology, Institute of Genetics and Developmental Biology, Chinese Academy of Sciences, 100101 Beijing, China

²University of Chinese Academy of Sciences, 100049 Beijing, China

³Center for Excellence in Animal Evolution and Genetics, Chinese Academy of Sciences, 650223 Kunming, China

⁴Department of Molecular and Cell Biology, Howard Hughes Medical Institute, and The Paul F. Glenn Center for Aging Research, University of California, Berkeley, Berkeley, CA 94720, USA

⁵These authors contributed equally

⁶Lead Contact

*Correspondence: ytian@genetics.ac.cn (Y.T.), dillin@berkeley.edu (A.D.)

<https://doi.org/10.1016/j.cell.2018.06.029>

SUMMARY

The mitochondrial unfolded protein response (UPR^{mt}) can be triggered in a cell-non-autonomous fashion across multiple tissues in response to mitochondrial dysfunction. The ability to communicate information about the presence of mitochondrial stress enables a global response that can ultimately better protect an organism from local mitochondrial challenges. We find that animals use retromer-dependent Wnt signaling to propagate mitochondrial stress signals from the nervous system to peripheral tissues. Specifically, the polyQ40-triggered activation of mitochondrial stress or reduction of *cco-1* (complex IV subunit) in neurons of *C. elegans* results in the Wnt-dependent induction of cell-non-autonomous UPR^{mt} in peripheral cells. Loss-of-function mutations of retromer complex components that are responsible for recycling the Wnt secretion-factor/MIG-14 prevent Wnt secretion and thereby suppress cell-non-autonomous UPR^{mt}. Neuronal expression of the Wnt ligand/EGL-20 is sufficient to induce cell-non-autonomous UPR^{mt} in a retromer complex-, Wnt signaling-, and serotonin-dependent manner, clearly implicating Wnt signaling as a strong candidate for the “mitokine” signal.

INTRODUCTION

Metazoan evolution required functional monitoring and communication of cellular stress across cells and tissues. The development of the nervous system plays a vital role in organismal homeostasis and coordinates diverse processes ranging from metabolism to circadian control of sleep. However, neurons appear to be one of the cell types most susceptible to the challenges of proteotoxic stress. How and why neurons succumb to

the adverse effects of neurodegenerative diseases caused by the imbalance of mal-folded proteins such as A β , α -synuclein, and polyglutamine repeats found in the huntingtin protein, while other non-neuronal cell types do not, is unknown. Even less well-understood is the mechanism for the age onset decline in processes responsible for the proper handling of the proteome and the proteostasis network, allowing the imbalance of mis-folded and toxic proteins that leads to neurodegeneration (Labbadia and Morimoto, 2015). However, many age-onset neurodegenerative diseases are accompanied by peripheral maladies that present as metabolic abnormalities and deficiencies in non-neuronal tissues (Cai et al., 2012; Duarte et al., 2013).

Studies in *C. elegans* have established that expression of the Huntington’s disease-causing polyglutamine expansion protein (Q40) in neurons results not only in neuronal detriment for the animal, but also peripheral decline in metabolic homeostasis, muscle function, and lifespan (Berendzen et al., 2016; Morley et al., 2002). Surprisingly, it is also associated with the induction of a protective stress response, the mitochondrial unfolded protein response (UPR^{mt}), which causes global alteration of transcription networks to maintain a functional mitochondrial proteome during challenges (Berendzen et al., 2016). Neuronal expressed Q40 associates with mitochondria, causing a local activation of the UPR^{mt} that is further communicated extracellularly across the animal to promote UPR^{mt} activation in non-neuronal, non-innervated cells and tissues. This process requires intact UPR^{mt} machinery, the active participation of serotonin, and the release of dense core vesicles (Berendzen et al., 2016). While serotonin is necessary for the cell-non-autonomous communication of UPR^{mt} stress response, it is not sufficient, suggesting other secreted factors might also be responsible for this signaling event.

Within *C. elegans*, the UPR^{mt} is activated when the transcription factor ATFS-1 translocates from mitochondria to the nucleus in response to mitochondrial perturbations (Nargund et al., 2012). A number of other proteins work together with ATFS-1 during UPR^{mt} activation, including the mitochondrial matrix protease ClpP, ubiquitin-like protein UBL-5, and the transcription

factor DVE-1 (Benedetti et al., 2006; Haynes et al., 2007). ATFS-1 and DVE-1/UBL-5 induce the expression of genes involved in mitochondrial quality control and cellular metabolism to restore proteostasis within mitochondria (Nargund et al., 2015). More recent studies have demonstrated the role of epigenetic regulation in UPR^{mt} induction. Two histone lysine demethylases (JMJD-1.2 and JMJD-3.1) that modify H3K27me2/me3 sites are necessary and sufficient for UPR^{mt} induction (Merkwirth et al., 2016). Chromatin remodeling is mediated by the MET-2/LIN-65 histone methyltransferases, which regulate UPR^{mt}-associated transcriptional networks (Tian et al., 2016).

Within metazoan, the induction of the UPR^{mt} can be coordinated across multiple tissues, preparing the entire organism to better cope with a locally sensed stress (Higuchi-Sanabria et al., 2018). For example, UPR^{mt} induction resulting from the knockdown of the mitochondrial electron transport chain (ETC) subunit *cco-1* (cytochrome c oxidase-1) in neurons is sensed and then reacted to by mitochondria located in the intestine, a physically distinct, non-innervated tissue, resulting in beneficial effects for the whole organism, including increased lifespan (Durieux et al., 2011). Further, the neuron-specific expression of the Q40 protein in *C. elegans* causes cell-non-autonomous induction of UPR^{mt} in the intestine (Berendzen et al., 2016).

Collectively, these findings have led to the mechanistic hypothesis that a factor, termed a mitokine, is generated in neurons experiencing mitochondrial stress, and is secreted, propagated, and subsequently perceived by cells of peripheral tissues to regulate organismal mitochondrial homeostasis. Humans with mitochondrial diseases, such as IOSCA (infantile onset spinocerebellar ataxia), suffer from muscle debilitation and produce excess levels of FGF21, a cytokine that enters and circulates in the blood (Suomalainen et al., 2011). Flies with disrupted muscle mitochondrial function have elevated levels of ImpL2 (an ortholog to human insulin-like growth factor binding protein 7), which systemically antagonizes insulin signaling, and prolongs lifespan (Owusu-Ansah et al., 2013). However, the molecular nature of a mitokine first perceived in the nervous system and sufficient to induce the mitochondrial stress response in distal cells has remained unknown.

Here, to identify a putative mitokine, we characterized *C. elegans* EMS mutants that are defective in cell-non-autonomous UPR^{mt} signaling but retain the ability for cell-autonomous UPR^{mt} induction. Intriguingly, within the 16 mutants identified, we found VPS-35, a retromer component, is required for the cell-non-autonomous UPR^{mt} induction through retrieval of the Wnt secretion factor, MIG-14. We further identified that the Wnt ligand, EGL-20, is not only essential, but also sufficient for cell-non-autonomous UPR^{mt} induction. Collectively, EGL-20 presents itself as a strong candidate to be a mitokine.

RESULTS

The Retromer Complex Is Required for Cell-Non-autonomous UPR^{mt} Induction

Neuronal expression of a polyglutamine repeat protein of 40 repeats (Q40) is sufficient to induce cell-non-autonomous UPR^{mt} signaling in peripheral, non-neuronal cells of *C. elegans* (Berendzen et al., 2016). UPR^{mt} activation can be monitored by

measuring the expression of the transcriptional UPR^{mt} reporter *hsp-6p::gfp* (Brignull et al., 2006). We performed an EMS mutagenesis screen using the *hsp-6p::gfp* reporter to identify mutants that suppress UPR^{mt} in peripheral cells of animals expressing neuronal Q40. Subsequently, we evaluated whether the mutants identified in this screen retained their ability to induce UPR^{mt} in response to cell-autonomous mitochondrial stress, such as *cco-1* RNAi delivered by bacterial feeding (Durieux et al., 2011; Houtkooper et al., 2013). Screening of 2,400 mutagenized genomes with these criteria yielded 16 mutant strains and *uth13*, the strain with the strongest suppression phenotype, was further characterized (Figure S1A).

Single nucleotide polymorphism (SNP) mapping and whole genome deep sequencing indicated that the *uth13* carries a mutation in the *vps-35* gene at the codon for amino acid 523 (CAA-TAA [Gln-Stop]) (Figure S1C). Using the deletion allele *vps-35(ok1880)*, we confirmed that *vps-35* was required for the induction of the *hsp-6p::gfp* reporter in the peripheral cells of animals expressing Q40 in neurons (Figures 1A and 1B). Western blot analysis confirmed that both *vps-35(uth13)* and *vps-35(ok1880)* mutant animals lost *hsp-6p::gfp* expression without any alteration of neuronal Q40 expression levels (Figures 1C and S1B). Furthermore, the induction of cell-autonomous UPR^{mt} in *vps-35* mutant animals was not affected when animals were treated with the cell autonomous stressor *cco-1* RNAi via bacterial feeding (Figures 1D and 1E). While multiple challenges to mitochondrial proteostasis in neurons can activate cell-non-autonomous UPR^{mt}, knockdown of the mitochondrial ETC subunit *cco-1* in neurons also activates UPR^{mt} in the peripheral tissue (Durieux et al., 2011). Intriguingly, we found that the *vps-35* mutation also suppressed the induction of *hsp-6p::gfp* expression in animals with neuronal *cco-1* knockdown (Figures 1F and 1G).

The non-autonomous nature of the unfolded protein response is not confined to the UPR^{mt}; the UPR^{ER} and UPR^{Cyt} also function in a cell-non-autonomous manner to coordinate stress responses across different tissues. For example, ectopic activation of the UPR^{ER} in neurons, by overexpression of XBP-1 s, activates the expression of *hsp-4p::gfp* reporter, a marker of UPR^{ER} expression, in the intestine of *C. elegans* (Ron and Walter, 2007; Taylor and Dillin, 2013). Similarly, overexpression of the heat shock transcription factor, HSF-1, in the nervous system induces the expression of the *sod-3p::gfp* reporter, a target gene of DAF-16, in the intestine (Douglas et al., 2015; Link et al., 1999). However, neither neuronal induction of the UPR^{ER} or UPR^{Cyt} activates the UPR^{mt}.

We found that *vps-35* was not involved in either the cell-autonomous or the cell-non-autonomous induction of the UPR^{ER} or UPR^{Cyt} (Figures S1D–S1G). Therefore, *vps-35* plays an essential and specific role in cell-non-autonomous UPR^{mt} communication. *vps-35* encodes an essential subunit of the retromer complex, a highly conserved multi-subunit complex that mediates the retrograde transport of cargo between endosomes and the trans-Golgi network (Bonifacino and Rojas, 2006). We additionally found that animals carrying mutations in two additional core retromer components (*vps-26* and *vps-29*) (Hierro et al., 2007) exhibited suppression phenotypes in animals expressing neuronal Q40 similar to those of the *vps-35* mutants

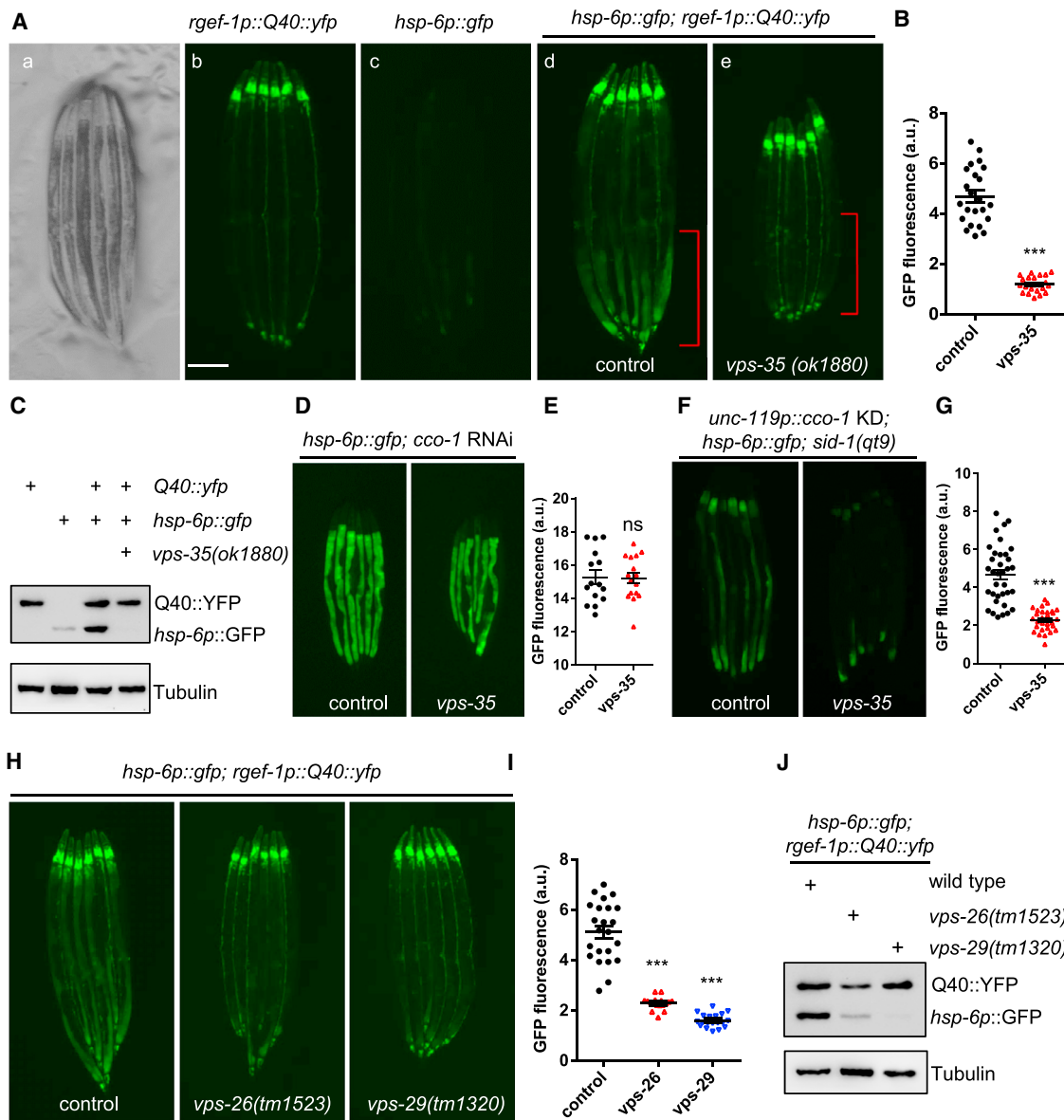


Figure 1. The Retromer Complex Is Required for Cell-Non-autonomous UPR^{mt} Induction in Animals Expressing Q40::YFP in Neurons

(A) Representative photomicrographs demonstrating: (a) bright field images of aligned, WT animals; (b) Q40::yfp expression in neurons; (c) *hsp-6p::gfp* expression in WT animals; (d) *hsp-6p::gfp* was upregulated in the intestine in day2 adult animals expressing neuronal Q40::YFP; (e) *hsp-6p::gfp* expression was suppressed in *vps-35* mutants. The posterior region of the intestine where *hsp-6p::gfp* is induced or suppressed is highlighted in (d) and (e). Scale bar, 250 μ m.

(B) Quantification of *hsp-6p::gfp* expression of the entire intestine in animals expressing Q40::YFP in neurons with the presence (d) or absence of the *vps-35* mutation (e) as shown in (A).

(C) Immunoblots of GFP expression in animals as indicated.

(D) Representative photomicrographs of *hsp-6p::gfp* animals with the presence or absence of the *vps-35* mutation grown on empty vector (EV) or with *cco-1* RNAi from hatching.

(E) Quantification of *hsp-6p::gfp* expression. The genotypes are as in (D).

(F) Representative photomicrographs of neuronal *cco-1* knockdown; *sid-1(qt9)*; *hsp-6p::gfp* animals with the presence or absence of *vps-35* mutation.

(G) Quantification of *hsp-6p::gfp* expression. The genotypes are as in (F).

(H) Representative photomicrographs of animals expressing neuronal Q40::YFP; *hsp-6p::gfp* in WT, *vps-26*, and *vps-29* animals.

(I) Quantification of *hsp-6p::gfp* expression. The genotypes are as in (H).

(J) Immunoblots of GFP expression in animals as indicated.

YFP can be recognized by the GFP antibody. Anti-tubulin serves as a loading control. *** $p < 0.0001$, ns denotes $p > 0.05$ via t test. Error bars, SEM $n \geq 15$ worms. See also Figure S1.

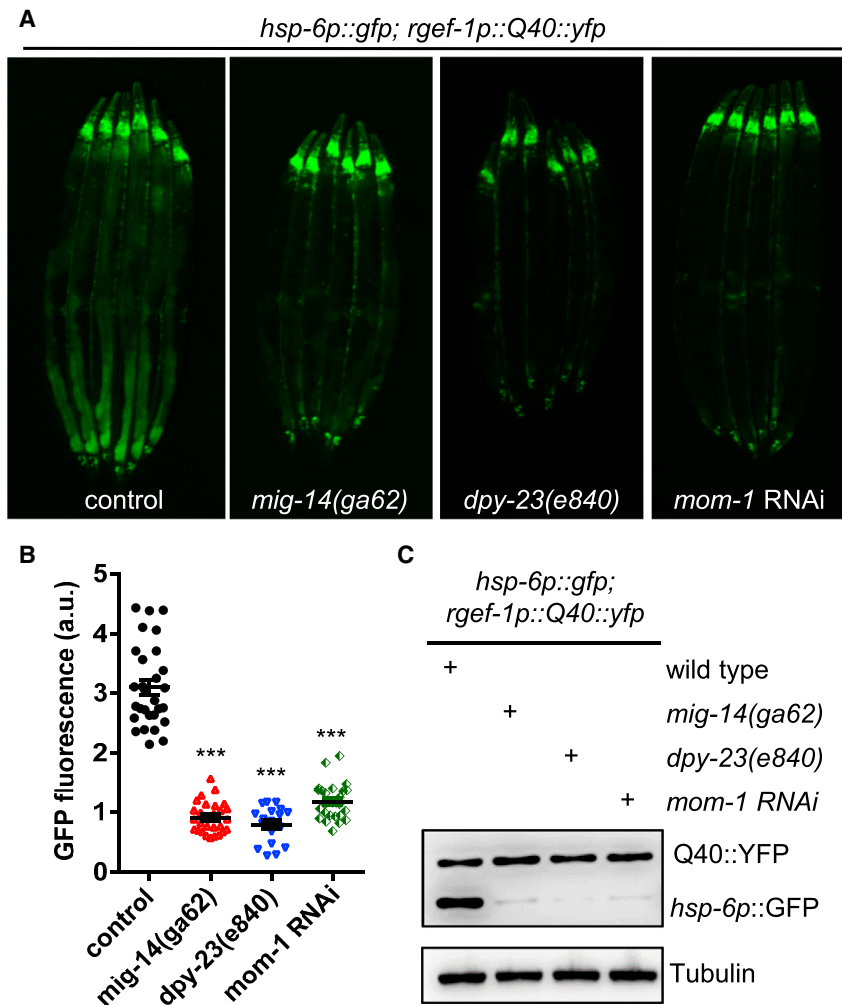


Figure 2. Retromer-Dependent Wnt Secretion Is Required for Cell-Non-autonomous UPR^{mt} Induction in Animals Expressing Q40::YFP in Neurons

(A) Representative photomicrographs of animals expressing neuronal Q40::YFP; *hsp-6p::gfp* in WT, *mig-14*, *dpy-23*, or *mom-1* RNAi animals. (B) Quantifications of the *hsp-6p::gfp* expression as shown in (A). *** $p < 0.0001$ via t test. Error bars, SEM $n \geq 20$ worms. (C) Immunoblots of GFP expression in animals as indicated. See also Figure S2.

not suppress the induction of cell-non-autonomous UPR^{mt} signaling in Q40 animals (Figures S2A and S2C). Likewise, the removal of mitochondrial fusion proteins *eat-3* and *fzo-1* also induced UPR^{mt} and did not suppress the induction of cell-non-autonomous UPR^{mt} of neuronal expressed Q40 animals (Figure S2B). Therefore, the role of the retromer complex in mitokine signaling does not appear to be linked to mitochondrial dynamics.

We next tested the retrieval function of the retromer complex, which is critical for efficient recycling of signaling receptors to allow proper transcellular signal transduction. We hypothesized that the observed loss of cell-non-autonomous UPR^{mt} signaling in the *vps-35* mutant was due to a defect in the retromer-mediated recycling of receptors that function in the cell-non-autonomous mitochondrial stress signaling pathway. We initially characterized receptors known to be retrieved by

(Figures 1H–1J). Thus, the retromer complex, and not solely *vps-35*, functions in the regulation of cell-non-autonomous UPR^{mt} signaling from the nervous system to the periphery.

Retrieval of the Wnt Secretion Factor, MIG-14, by the Retromer Complex Is Required for Cell-Non-autonomous UPR^{mt} Signaling

The retromer complex mediates at least two essential aspects of cellular biology: the regulation of mitochondrial dynamics and the retrieval of various cargo proteins from endosomes to the trans-Golgi network (e.g., glutamate, transforming growth factor β [TGF- β], Wnt, and phagocytic secretion factors) (Belenkaya et al., 2008; Chen et al., 2010; Gleason et al., 2014; Zhang et al., 2012). We first tested the role of the retromer complex in mitochondrial dynamics. Here, VPS35 facilitates the degradation of the dynamin-like protein, DLP1, via the mitochondrial-derived vesicle pathway (Wang et al., 2016). We examined the effects of a loss-of-function mutation and of overexpression of *drp-1*, the *C. elegans* DLP1 homolog (Labrousse et al., 1999). The *drp-1(tm1108)* mutant and the *drp-1* overexpression strain both induced the expression of *hsp-6p::gfp* reporter and did

the retromer complex and found that the Wnt secretion factor, MIG-14, was required for induction of the *hsp-6p::gfp* reporter in animals expressing Q40 in neurons (Figures 2A and 2B). In contrast, the glutamate receptor GLR-1, the phagocytic receptor CED-1, and the TGF- β receptor SMA-6, which are also retrieved by the retromer complex, are not involved in cell-non-autonomous UPR^{mt} signaling (Figure S2C).

Studies across multiple organisms have demonstrated that Wnt ligands are post-translationally modified with lipids (Clevers and Nusse, 2012). Lipidation of Wnt ligands occurs in the ER and is catalyzed by the enzyme porcupine (*mom-1* in *C. elegans*) (Rochelleau et al., 1997). The Wnt secretion factor, MIG-14, can then bind these modified Wnt ligands and transport them from the Golgi to the cell surface (Bänziger et al., 2006). After Wnt ligands have been released to the extracellular space, MIG-14 becomes internalized via the clathrin adaptor DPY-23/AP2-mediated endocytosis pathway (Pan et al., 2008). Subsequently, the retromer-dependent retrieval pathway delivers MIG-14 back to the Golgi, where it becomes available for further Wnt secretion (Yang et al., 2008). We found that loss of the DPY-23/AP2 adaptor in *dpy-23* mutants resulted in suppression of the

mitokine signaling that phenocopied the *mig-14* mutant animals (Figures 2A and 2B). We also found that lipid modification of Wnt is essential for the mitokine signaling induction: *mom-1* RNAi strongly suppressed induction of the *hsp-6p::gfp* reporter in neurons of Q40 animals (Figures 2A and 2B). Western blot analysis verified that *hsp-6p::GFP* levels were dramatically reduced in *mig-14*, *dpy-23*, and *mom-1* mutants as compared to wild-type (WT) animals expressing neuronal Q40 (Figure 2C). Moreover, we observed no differences in the induction of cell-autonomous UPR^{mt} when we fed *cco-1* RNAi bacteria to *mig-14*, *dpy-23*, and *mom-1* mutants compared to control animals (Figure S2D). Furthermore, we overexpressed *mig-14* in *vps-35* mutant animals expressing neuronal Q40 and found that *mig-14* overexpression partially rescued the *hsp-6p::gfp* suppression phenotypes in *vps-35* mutants. Our observation that excess MIG-14 ameliorated *vps-35* suppression on UPR^{mt} induction is consistent with the prediction that retromer-dependent MIG-14 recycling is essential for mitokine signaling (Figure S2E).

The Wnt Ligand, EGL-20, Is Required for Cell-Non-autonomous UPR^{mt} Signaling

We performed a candidate screen against all known Wnt ligands in *C. elegans* (*egl-20*, *lin-44*, *cwn-1*, *cwn-2*, and *mom-2*) (Shackleford et al., 1993; Herman et al., 1995; Maloof et al., 1999; Rocheleau et al., 1997; Thorpe et al., 1997) for their role in UPR^{mt} signaling. *egl-20(n585)* was the only Wnt ligand mutation able to suppress the induction of cell-non-autonomous UPR^{mt} signaling of animals expressing neuronal Q40 (Figures 3A and 3B). The other Wnt ligand mutants did not affect either the cell autonomous or cell-non-autonomous UPR^{mt} induction (Figures S3A–S3C). Western blot analysis verified that *hsp-6p::GFP* levels were dramatically reduced in *egl-20* mutants compared to the control animals expressing neuronal Q40 (Figure 3C). Furthermore, we measured the endogenous *hsp-6* mRNA levels and found that it was also dramatically reduced by the loss of *egl-20* in the neuronal expressed Q40 animals (Figure S3D).

To further measure UPR^{mt} induction, we followed the nuclear localization of the DVE-1 transcription factor using the DVE-1::GFP fusion protein reporter. DVE-1 translocates to the nucleus in response to mitochondrial stress to induce the UPR^{mt} (Haynes et al., 2007). We observed robust nuclear accumulation of DVE-1::GFP in the intestinal cells of neuronal Q40 animals, but only moderate DVE-1::GFP nuclear accumulation in *egl-20* mutants (Figures 3D and 3E). In contrast, when *cco-1* RNAi producing bacteria were fed to the *egl-20* mutants, the *hsp-6p::gfp* induction was comparable to that of wild-type animals (Figures 3F and 3G). Therefore, *egl-20* is not required for cell autonomous UPR^{mt} signaling, much like the retromer complex, DPY-23/AP2, and MIG-14. Of the five Wnt ligands found in *C. elegans*, EGL-20 is the only Wnt ligand that can act across the entire length of the animal, whereas the other four act more proximal to their site of secretion (Hardin and King, 2008). Furthermore, we found that the *egl-20* mutant also strongly suppressed the induction of cell-non-autonomous UPR^{mt} upon neuronal *cco-1* RNAi (Figures 3H and 3I). Taken together, EGL-20 is specifically required for the cell-non-autonomous UPR^{mt} signaling from the nervous system to the periphery.

Neuronal Expression of *egl-20* Is Sufficient for the Induction of Mitokine Signaling

Because *egl-20* is required for cell-non-autonomous communication of the UPR^{mt}, we tested whether tissue-specific expression of *egl-20* was sufficient to induce the UPR^{mt} cell-non-autonomously. To this end, we generated transgenic strains expressing *egl-20* with pan-neuronal promoter (*rgef-1p*, two independent lines) or in the intestine (*gly-19p*, two independent lines). Intriguingly, expression of *egl-20* in either neurons or the intestine was sufficient for the induction of *hsp-6p::gfp* reporter and for the nuclear translocation of DVE-1::GFP reporter (Figures 4A–4F, S4A–S4C, and S4E). Likewise, expression of *egl-20* in the Wnt-producing cells was sufficient to induce cell-non-autonomous UPR^{mt} signaling (Figures 4G–4I). However, expression of *egl-20* in the body wall muscle (*myo-3p*), pharyngeal muscle (*myo-2p*), or hypodermal cells (*lin-26p*) failed to activate the expression of the *hsp-6p::gfp* reporter (Figure S4D). Furthermore, neither the *hsp-4p::gfp* reporter (UPR^{ER}) nor the *hsp-16.2p::gfp* reporter (UPR^{Cvt}) were induced by neuronal or intestinal Wnt/EGL-20 expression, indicating that expression of Wnt/EGL-20 had a specific effect on mitokine signaling (Figures S4F and S4G).

Ectopic induction of mitokine signaling by *egl-20* expression required core components of the UPR^{mt} response. RNAi against *atfs-1* or *dve-1* strongly suppressed *hsp-6p::gfp* induction in both neuronal and intestinal *egl-20* overexpression animals (Figures 4J, 4K, S4I, and S4J). Additionally, RNAi against the epigenetic factors *lin-65* and the demethylase *jmjd-1.2*, both of which specifically function in UPR^{mt} signaling (Merkwirth et al., 2016; Tian et al., 2016), also strongly suppressed *hsp-6p::gfp* induction in both neuronal and intestinal *egl-20* expression animals (Figures 4J, 4K, S4I, and S4J).

The crystal structure of the *Xenopus* Wnt8 (XWnt8) in complex with mouse Frizzled-8 (Fz8) cysteine-rich domain (CRD) reveals a two-domain Wnt structure that comprises an N-terminal α -helical domain (NTD) that contains the lipid-modified sites and a C-terminal cysteine-rich domain (CTD, also termed “mini-Wnt”) that autonomously engages the Fz8-CRD in a receptor-specific manner (Janda et al., 2012). Interestingly, neuronal expression of the C-terminal end of EGL-20 (mini-Wnt) was sufficient for *hsp-6p::gfp* induction, whereas N-terminal EGL-20 failed to induce *hsp-6p::gfp* expression (Figures 4L and 4M).

To characterize the physiological function of *egl-20* overexpression, we performed mitochondrial morphology analyses. Mitochondria formed more fragmented structures in muscle cells of the posterior region of animals with *egl-20* overexpression than in the WT control animals using the *myo-3p::GFP(mit)* reporter (Figure S4H). Furthermore, both neuronal and intestinal *egl-20* expressing animals induced greater lifespan extension than did the WT animals (Figure 4N; Table S1).

β -Catenin and the TCF Transcription Factor Are Required for Cell-Non-autonomous UPR^{mt} Signaling

Wnt ligands engage with various receptors to activate multiple downstream signaling pathways. Wnt signaling pathways can be classified as either canonical (β -catenin-dependent) or non-canonical (β -catenin-independent) (Komiya and Habas, 2008). In the absence of a Wnt ligand, the destruction complex (known

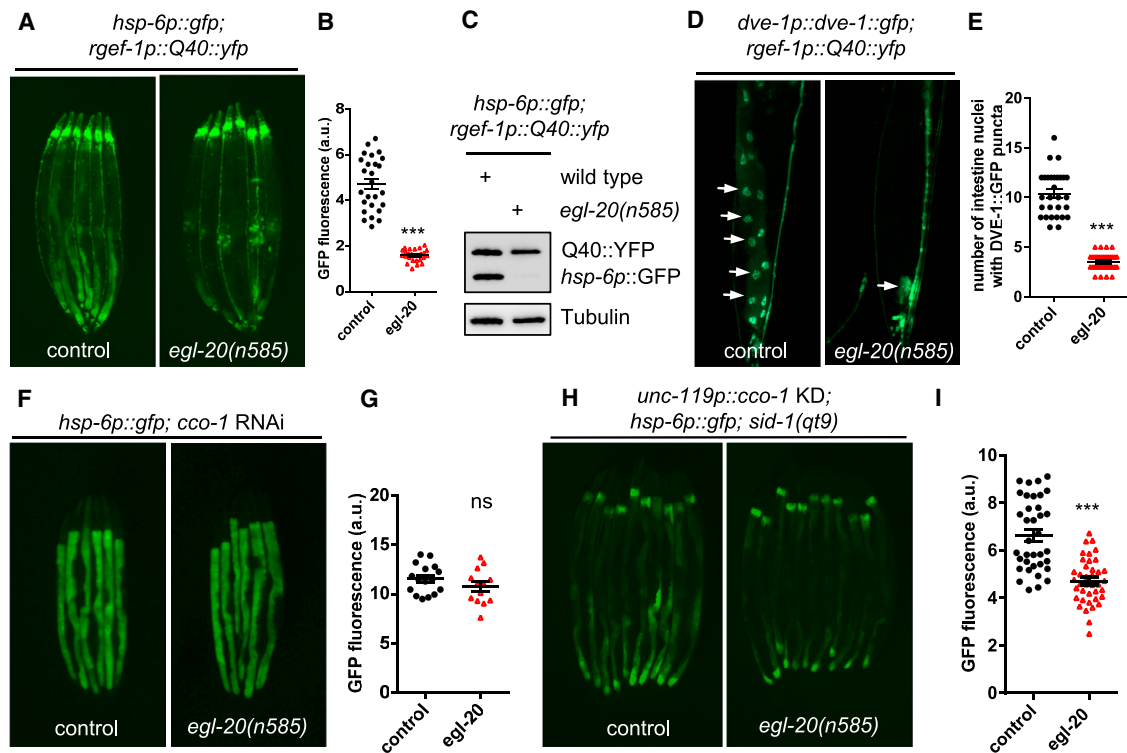


Figure 3. Wnt Ligand/EGL-20 Is Required for Cell-Non-autonomous UPR^{mt} Induction in Animals with Q40::YFP Expression in Neurons

(A) Representative photomicrographs of D2 adult animals expressing neuronal Q40::YFP; *hsp-6p::gfp* in WT or *egl-20* animals.
 (B) Quantification of *hsp-6p::gfp* expression. The genotypes are as in (A).
 (C) Immunoblots of GFP expression. The genotypes are as in (A).
 (D) Representative photomicrographs of D2 adult animals expressing neuronal Q40::YFP; DVE-1::GFP in WT and *egl-20* animals. Arrows highlight the DVE-1::GFP signal localized in the intestinal nuclei.
 (E) Quantification of the number of intestinal nuclei with DVE-1 puncta. The genotypes are as in (D).
 (F) Representative photomicrographs of D1 animals expressing *hsp-6p::gfp* in WT or *egl-20* animals grown on EV or *cco-1* RNAi from hatching.
 (G) Quantification of *hsp-6p::gfp* expression. The genotypes are as in (F).
 (H) Representative photomicrographs of *hsp-6p::gfp* expression in neuronal specific *cco-1* RNAi animals in WT or *egl-20* background.
 (I) Quantification of *hsp-6p::gfp* expression. The genotypes are as in (H).
 ****p* < 0.0001, ns denotes *p* > 0.05 via t test. Error bars, SEM *n* ≥ 15 worms.
 See also [Figure S3](#).

as APC/Axin/CK1/GSK3 β) phosphorylates cytosolic β -catenin, ultimately resulting in the degradation of β -catenin by the proteasome. Binding of a Wnt ligand to a Frizzled/LRP-5/6 receptor causes the recruitment of the destruction complex leading to the stabilization of β -catenin. Stabilized β -catenin can then enter the nucleus and interact with the TCF/LEF transcription factor to activate the expression of Wnt target genes (Clevers, 2006).

To determine which downstream signaling pathways of Wnt activation are involved in mitokine signaling, we analyzed the requirement for each of the Wnt receptors. The *C. elegans* genome encodes multiple genes for Wnt-Frizzled receptors, including *lin-17*, *mom-5*, *mig-1*, and *cfz-2* (Rocheleau et al., 1997; Ruvkun and Hobert, 1998; Sawa et al., 1996). Using the *mig-1(e1787)* mutation, we found that loss of *mig-1*, although not of the other Wnt receptor mutants, resulted in significantly lower expression of the *hsp-6p::gfp* reporter in neuronal Q40 animals (Figures 5A–5C, and S5A). Furthermore, RNAi-mediated

knockdown of *bar-1* (β -catenin) or *pop-1* (TCF/LEF transcription factor) resulted in strong suppression of *hsp-6p::gfp* induction in the animals expressing neuronal Q40 (Figures 5A–5C). The roles of *mig-1*, *bar-1*, and *pop-1* appear specific to mitokine signaling because mutations in any of the three genes did not block induction of *hsp-6p::gfp* induction when animals were fed *cco-1* RNAi bacteria (Figure S5B). To test whether stabilization of β -catenin was sufficient to induce UPR^{mt}, we disrupted the activity of *pry-1*, a component of the destruction complex that targets β -catenin for degradation in the absence of Wnt signaling (Korswagen et al., 2002). As expected, we observed nuclear accumulation of the DVE-1::GFP fusion protein in *pry-1* RNAi animals (Figures S5C and S5D). Furthermore, disruption of the E3 ligase *lin-23*, which is required for β -catenin degradation (Dreier et al., 2005), resulted in robust ectopic induction of the *hsp-6p::gfp* reporter (Figures S5E and S5F).

To understand whether Wnt signaling is required during development to mediate cell-non-autonomous UPR^{mt} induction, we

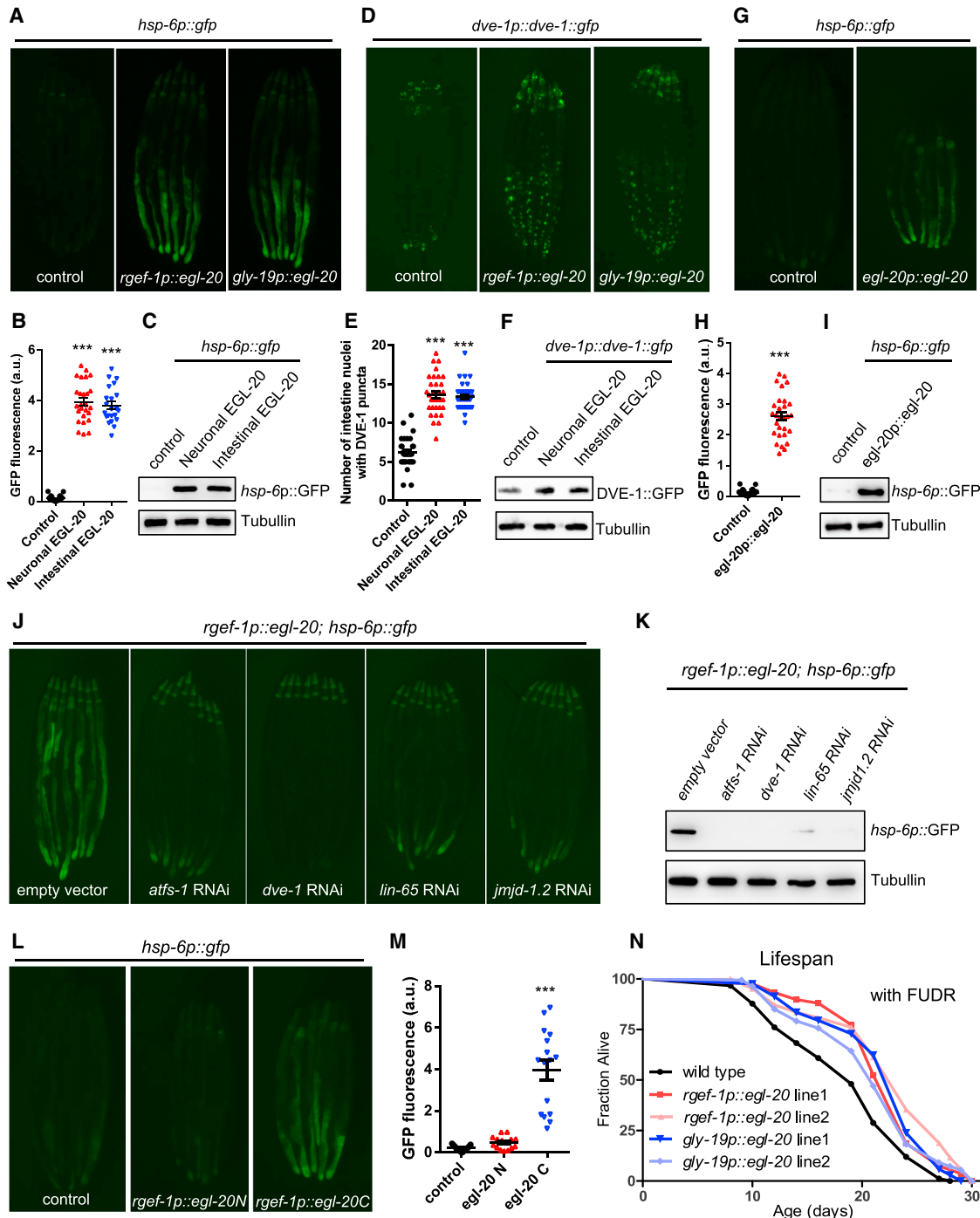


Figure 4. Expression of Wnt Ligand/EGL-20 Is Sufficient to Induce UPR^{mt} in Both Cell-Autonomous and Cell-Non-autonomous Manners

- (A) Representative photomicrographs of *hsp-6p::gfp* reporter animals in WT, *rgef-1p::egl-20* (neuronal), and *gly-19p::egl-20* (intestinal) background. (B) Quantification of *hsp-6p::gfp* expression. The genotypes are as in (A). (C) Immunoblot of *hsp-6p::gfp* expression. The genotypes are as in (A). (D) Representative photomicrographs of DVE-1::GFP reporter animals in WT, *rgef-1p::egl-20*, and *gly-19p::egl-20* background. (E) Quantification of the number of intestinal nuclei with DVE-1 puncta. The genotypes are as in (D). (F) Immunoblot of DVE-1::GFP expression. The genotypes are as in (D). (G) Representative photomicrographs of *hsp-6p::gfp* reporter animals in WT or *egl-20p::egl-20::mCherry* background. (H) Quantification of *hsp-6p::gfp* expression. The genotypes are as in (G). (I) Immunoblot of *hsp-6p::gfp* expression. The genotypes are as in (G). (J) Representative photomicrographs of *hsp-6p::gfp* reporter animals in *rgef-1p::egl-20; hsp-6p::gfp* background with various RNAi treatments. (K) Immunoblot of *hsp-6p::gfp* expression. The genotypes are as in (J). (L) Representative photomicrographs of *hsp-6p::gfp* reporter animals in *rgef-1p::egl-20N* and *rgef-1p::egl-20C* backgrounds. (M) Quantification of *hsp-6p::gfp* expression. The genotypes are as in (L). (N) Lifespan curve with FUDR for wild type and various *rgef-1p::egl-20* and *gly-19p::egl-20* lines.

(legend continued on next page)

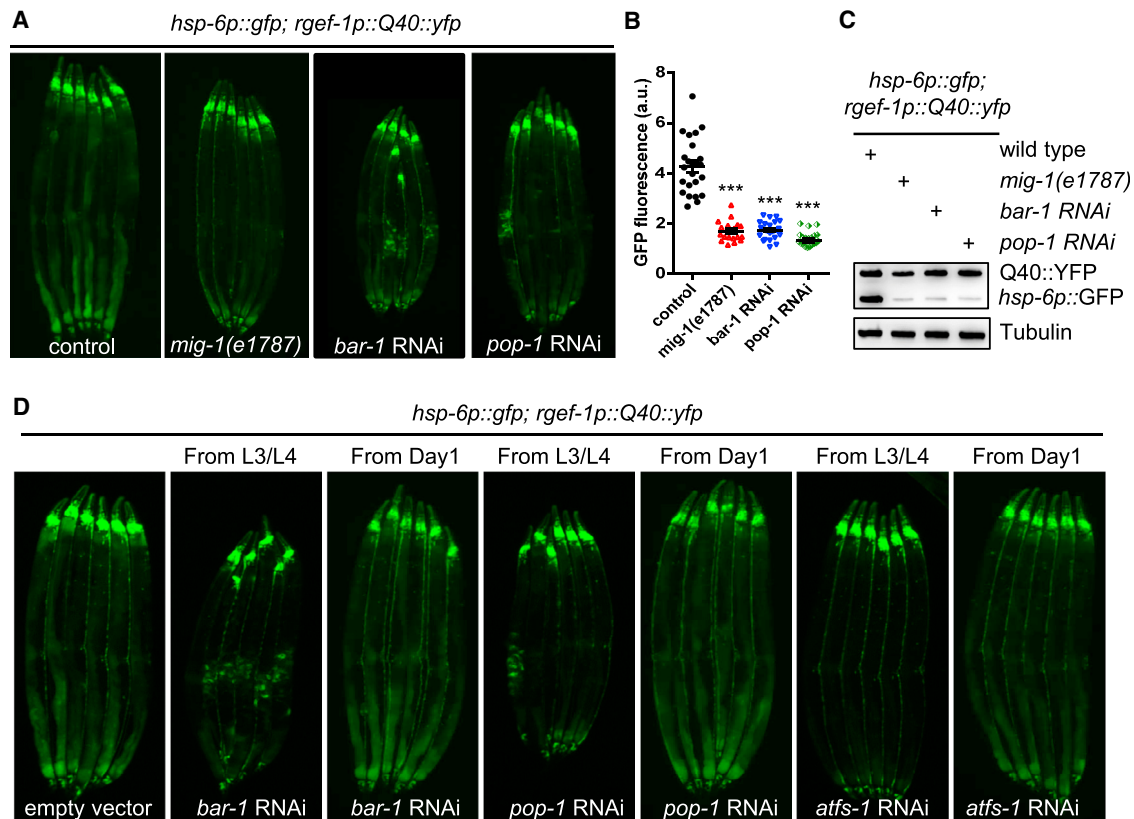


Figure 5. The Canonical Wnt/ β -Catenin Signaling Pathway Is Required for Cell-Non-autonomous UPR^{mt} Induction in Animals Expressing Q40::YFP in Neurons

(A) Representative photomicrographs of neuronal Q40::YFP; *hsp-6p::gfp* expressing animals in WT, *mig-1*, *bar-1* RNAi, or *pop-1* RNAi background. (B) Quantification of *hsp-6p::gfp* expression. The genotypes are as in (A). *** $p < 0.0001$ via t test. Error bars, SEM $n \geq 20$ worms. (C) Immunoblots of GFP expression. The genotypes are as in (A). (D) Representative photomicrographs of neuronal Q40::YFP; *hsp-6p::gfp* expressing animals transferred to RNAi plates either from L3/L4 stages or D1 adulthood. See also Figure S5.

tested the timing requirement of *bar-1*, *pop-1*, and *atfs-1* in animals expressing Q40 in neurons. Animals in which RNAi was induced from the L3/L4 stages during late development were able to strongly suppress cell-non-autonomous UPR^{mt} induction. In contrast, animals treated with RNAi during adulthood failed to suppress UPR^{mt} induction. These results indicate that a critical timing window during the L3/L4 stages of early development is essential for cell-non-autonomous UPR^{mt} induction (Figure 5D). This observation is very consistent with previous timing requirements found for mitokine signaling (Dillin et al., 2002; Durieux et al., 2011; Merkwirth et al., 2016).

Induction of Cell-Non-autonomous UPR^{mt} Signaling upon Neuronal Wnt/EGL-20 Expression Requires Retromer and Canonical Wnt Signaling

The retromer complex enables Wnt molecules to be secreted for long range transduction of Wnt signals (Coudreuse et al., 2006). We tested whether VPS-35 is also required for cell-non-autonomous UPR^{mt} activation when EGL-20 is expressed in neurons. Intriguingly, in the *vps-35* mutant, the induction of UPR^{mt} was strongly suppressed in animals expressing *egl-20* in neurons but was unaffected in animals expressing *egl-20* in the intestine (Figures 6A–6F). Notably, *bar-1* and *pop-1*, two downstream

(J) Representative photomicrographs of *rgef-1p::egl-20*; *hsp6p::gfp* reporter animals grown on EV, *atfs-1*, *dve-1*, *lin-65*, or *jmjd-1.2* RNAi from hatching.

(K) Immunoblot of *hsp-6p::gfp* expression. The genotypes are as in (J).

(L) Representative photomicrographs of *hsp-6p::gfp* reporter animals in WT, *rgef-1p::egl-20N(1-720)::mCherry*, or *rgef-1p::egl-20C(721-1182)::mCherry* background.

(M) Quantification of *hsp-6p::gfp* expression. The genotypes are as in (L).

(N) Overexpression of *egl-20* in neurons or in the intestine extends *C. elegans* lifespan. Lifespan analysis of two independent transgenic lines of *rgef-1p::egl-20* or *gly-19p::egl-20* expressing animals compared to WT animals. See also Table S1.

*** $p < 0.0001$ via t test. Error bars, SEM $n \geq 20$ worms.

See also Figure S4.

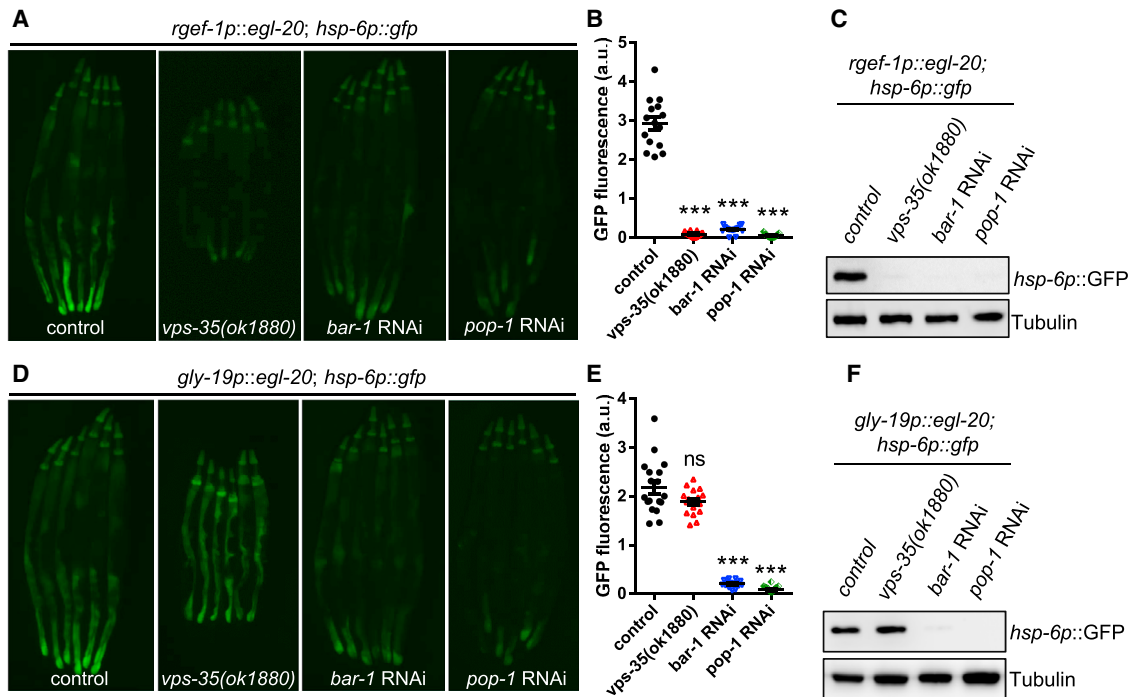


Figure 6. The Induction of Cell-Non-autonomous UPR^{mt} Signaling upon Neuronal Wnt/EGL-20 Expression Is Dependent on the Retromer Complex and Canonical Wnt Signaling

(A) Representative photomicrographs of *rgef-1p::egl-20; hsp-6p::gfp* reporter animals in WT, *vps-35*, *bar-1* RNAi, or *pop-1* RNAi background.

(B) Quantification of *hsp-6p::gfp* expression. The genotypes are as in (A).

(C) Immunoblot of GFP expression. The genotypes are as in (A).

(D) Representative photomicrographs of *gly-19p::egl-20; hsp-6p::gfp* reporter animals in WT, *vps-35*, *bar-1* RNAi, or *pop-1* RNAi background.

(E) Quantification of *hsp-6p::gfp* expression. The genotypes are as in (D).

(F) Immunoblot of GFP expression. The genotypes are as in (D).

****p* < 0.0001 via *t* test. Error bars, SEM *n* ≥ 15 worms.

See also Figure S6.

regulators of Wnt signaling, are required for the induction of UPR^{mt} signaling in animals with neuronal or intestinal expression of Wnt/EGL-20 (Figures 6A–6F). Collectively, these results indicate that canonical Wnt/β-catenin signaling is required for both local and long range induction of EGL-20-induced mitokine signaling, while retromer activity is only essential for long range UPR^{mt} signaling originating from the nervous system.

To identify which tissue is essential for mediation of cell-non-autonomous UPR^{mt} by the retromer complex, we performed rescue experiments to induce *vps-35* expression using tissue-specific promoters in the *vps-35* mutant animals. Expression of *vps-35* in Wnt/EGL-20 producing cells strongly rescued the suppression of the *hsp-6p::gfp* reporter in the *vps-35* mutants with neuronal Q40 expression (Figures S6A and S6B). However, expression of *vps-35* in neurons or in the intestine failed to restore cell-non-autonomous UPR^{mt} signaling in the *vps-35* mutants (Figures S6A and S6B). Collectively, these results suggest that the retromer complex is required in Wnt-producing cells to mediate mitokine signaling.

Serotonin Is Essential for EGL-20 Mitokine Signaling

Serotonin can define non-autonomous from autonomous UPR^{mt} induction. Consistent with the role of serotonin for cell-non-

autonomous UPR^{mt} induction in animals expressing Q40 in neurons (Berendzen et al., 2016), mutations in tryptophan hydroxylase (*tph-1*), a key enzyme for serotonin synthesis, completely suppressed the induction of the *hsp-6p::gfp* reporter in the animals expressing *egl-20* in neurons (Figures 7A–7C), whereas it only slightly suppressed the induction of the *hsp-6p::gfp* reporter in the animals expressing *egl-20* in the intestine (Figures 7D–7F). Importantly, the addition of serotonin rescued the suppression caused by the *tph-1* mutation in animals expressing *egl-20* in neurons (Figures 7G–7J). Serotonin released from neurons may exert its function by targeting a serotonin receptor. We therefore tested mutations within the four serotonin receptors (*ser-1*, *ser-4*, *ser-7*, and *mod-1*) found in *C. elegans* (Chase and Koelle, 2007), and they had no effect on cell-non-autonomous UPR^{mt} signaling (Figures S7A and S7B). Moreover, expression of *egl-20* solely in serotonergic neurons was sufficient to induce mitokine signaling in the periphery (Figures 7K and 7L).

DISCUSSION

The development and survival of multicellular organisms relies to a large extent on the ability of cells to communicate via

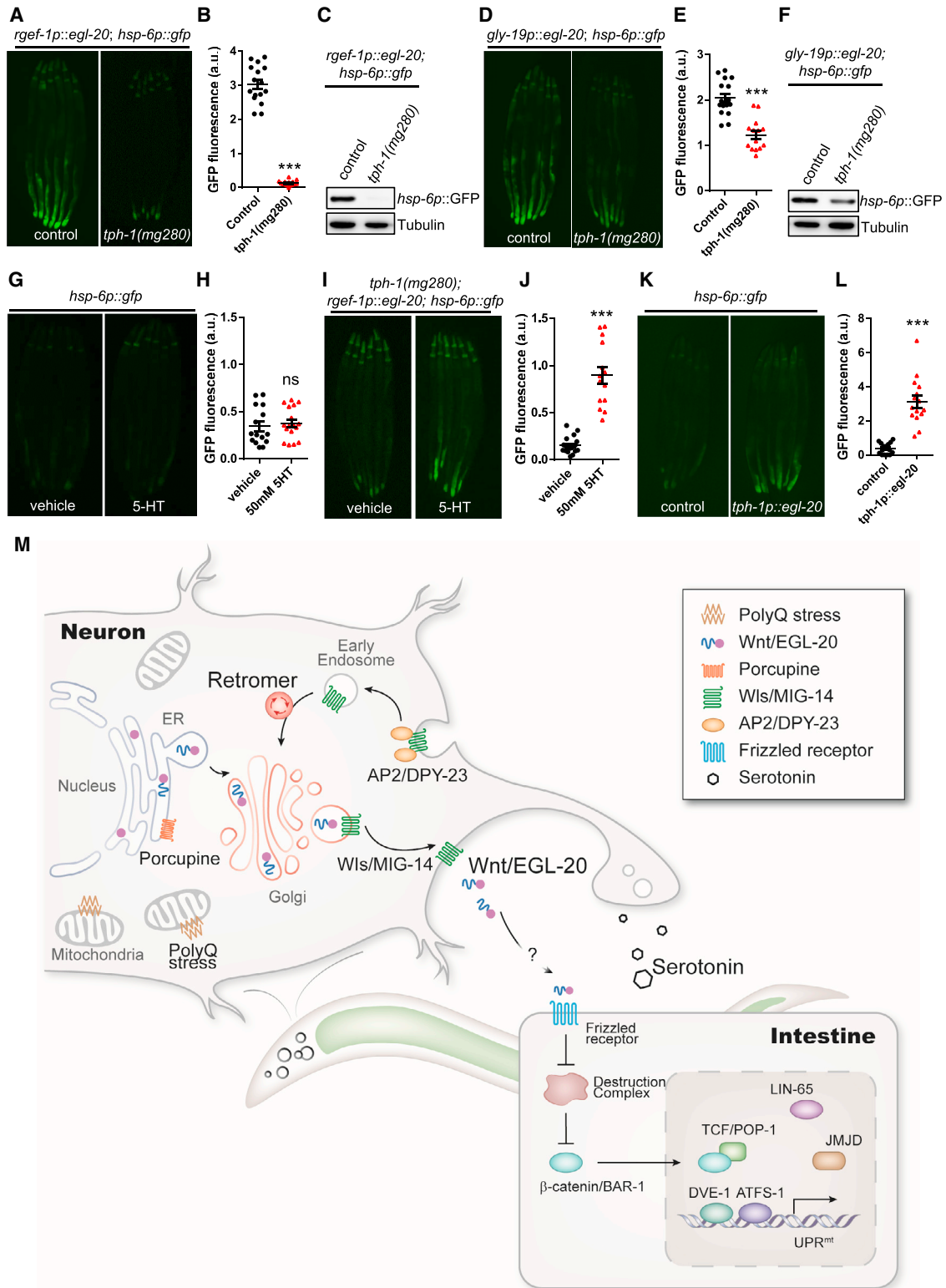


Figure 7. Serotonin Is Required for the Cell-Non-autonomous UPR^{mt} Induction upon Neuronal Wnt/EGL-20 Expression

(A) Representative photomicrographs of *rgef-1p::egl-20; hsp-6p::gfp* animals in WT or *tph-1* background.

(B) Quantification of *hsp-6p::gfp* expression. The genotypes are as in (A).

(C) Immunoblot of *hsp-6p::gfp* expression. The genotypes are as in (A).

(legend continued on next page)

extracellular signals, such as the well-characterized Wnt signaling pathway (Nusse and Clevers, 2017). This pathway directs processes as diverse as embryonic cell division, limb development, and neuronal patterning and migration (Wodarz and Nusse, 1998), as well as the regulation of stem cell maintenance and differentiation (Reya and Clevers, 2005). Aberrant Wnt activation has been implicated in several types of cancer (Logan and Nusse, 2004). Additionally, it has been proposed that Wnt signaling functions in a protective role against neurodegenerative diseases (Inestrosa and Arenas, 2010). However, very few reports have linked Wnt signaling to mitochondrial function (Yoon et al., 2010). We found that retromer-dependent Wnt signaling is required for the induction of cell-non-autonomous UPR^{mt} from the nervous system to the periphery.

Given the large number of proteins known to depend upon the retromer complex for endosomal sorting, it is not surprising that retromer dysfunction has been implicated in a number of human diseases, including forms of Alzheimer's and Parkinson's diseases (Wang and Bellen, 2015). The present study broadens our understanding of the functional roles of the retromer complex in transducing intercellular signals by demonstrating that the retromer complex is directly involved in a cell-non-autonomous mitochondrial stress response—UPR^{mt}.

EGL-20 is the only Wnt in *C. elegans* that has been demonstrated to signal over a long distance (Hardin and King, 2008; Whangbo and Kenyon, 1999). During early larval development, EGL-20 is expressed by a group of cells located at the posterior end of the animal (Gleason et al., 2006). The retromer complex and MIG-14 function in EGL-20-producing cells to allow the formation of an EGL-20 gradient along the anteroposterior axis during the larval stages (Coudreuse et al., 2006) (Figure S7C). However, it remains unclear whether neuronal mitochondrial stress can activate Wnt signaling and induce UPR^{mt} over a distance. Due to the very low expression level of *egl-20* in *C. elegans*, no significant differences were observed in expression levels of either the endogenous *egl-20* mRNA level or the expression of an *egl-20p::egl-20::mCherry* translational reporter in animals expressing Q40 in neurons as compared to WT animals (Figures S7D, S7E, and S7H). Additionally, we found that some Wnt target genes (Gorrepati et al., 2015; Jackson et al., 2014) are strongly upregulated in animals expressing neuronal Q40 (Figure S7F). Notably, our results appear to suggest that the overall level of Wnt/EGL-20 might not be upregulated upon mitochondrial stress; however, either transient or undetectable local upregula-

tion of Wnt signaling could still be occurring in cells experiencing mitochondrial stress or the localization/secretion of EGL-20 could also be affected during neuronal mitochondrial stress.

While EGL-20/Wnt expression is limited in early larval stages, its potential expression in neurons has not been extensively explored. Here, we carefully examined the distribution of EGL-20. The *egl-20p::mCherry* reporter showed the co-localization of the signal with the ventral nerve cord in the posterior region of *C. elegans* (Figure S7G). Furthermore, the EGL-20::mCherry fusion protein formed aggregates along or co-localized with the ventral and dorsal nerve cord (Figure S7G), indicating a potential function for Wnt/EGL-20 in neurons.

Wnt-receptor interactions can elicit a variety of intracellular responses, the best-known of which results in the activation of β -catenin, which was demonstrated to regulate mitokine signaling in this study. β -catenin is frequently found to be hyperactivated in most intestinal cancers and in a variety of other maladies. Further studies of the interactions between β -catenin and the key regulators of the UPR^{mt} pathway may elucidate new therapeutic interventions to cancers.

The mitokine hypothesis was put forth to explain how RNAi of mitochondrial ETC complex in the nervous system could coordinate whole body aging and induction of the UPR^{mt}. Further studies on this potentially unique signaling system determined parameters for such a mitokine molecule. The mitokine should depend upon serotonin and the downstream UPR^{mt} factors as well as the newly identified LIN-65 chromatin remodeling complex (Tian et al., 2016). Furthermore, the mitokine should be sufficient to induce UPR^{mt} even in the absence of mitochondrial stress, be able to originate from nerve tissues, and able to act at a distance. Our analysis and mutant screen show that *egl-20*, known as Wnt16b in humans, follows these mandates. One of the most difficult rules to comply with is that of sufficiency. Few molecules responsible for stress induction are sufficient. Such molecules include HSF1, controlling the heat shock response, *xbp-1* for the ER stress response, and PHF-8 dictating the UPR^{mt} response, all of which are transcription factors or chromatin remodelers. Therefore, the description of a Wnt ligand which can play a necessary, specific, and sufficient role in mitokine signaling provides important knowledge in the biology of transcellular stress responsiveness.

In summary, we discovered that the retromer complex is essential for cell-non-autonomous UPR^{mt}, and our subsequent identification and characterization of the proteins recycled by

(D) Representative photomicrographs of *gly-19p::egl-20; hsp-6p::gfp* transgenic animals in WT or *tph-1* background.

(E) Quantification of *hsp-6p::gfp* expression. The genotypes are as in (D).

(F) Immunoblot of *hsp-6p::gfp* expression. The genotypes are as in (D).

(G) Representative photomicrographs of *hsp-6p::gfp* expression in animals treated with vehicle control or 50mM serotonin (5-HT).

(H) Quantification of *hsp-6p::gfp* expression. The genotypes are as in (G).

(I) Representative photomicrographs of *hsp-6p::gfp* expression in neuronal Q40; *tph-1* expressing animals treated with vehicle control or 50mM 5-HT.

(J) Quantification of *hsp-6p::gfp* expression. The genotypes are as in (I).

(K) Representative photomicrographs of *hsp-6p::gfp* reporter animals in WT and *tph-1p::egl-20* background.

(L) Quantification of *hsp-6p::gfp* expression. The genotypes are as in (K).

(M) Model of the mitokine signaling pathway. Q40 specifically binds to mitochondria in neurons, initiating a signaling cascade across tissues that requires retromer-dependent Wnt secretion, canonical Wnt signaling, serotonin, and functional components of the UPR^{mt} to ensure cell-non-autonomous UPR^{mt} induction in peripheral tissues.

***p < 0.0001 via t test. Error bars, SEM n \geq 15 worms.

See also Figure S7.

the retromer complex demonstrated that the Wnt signaling pathway is also required for this cellular response to mitochondrial stress. Further, we found that Wnt expression is sufficient to induce the UPR^{mt} in both a cell-autonomous and a cell-non-autonomous manner, thereby identifying Wnt as a strong candidate for the proposed “mitokine” signal. In keeping with the recently discovered role of the neurotransmitter serotonin in mitochondrial function, we also found that serotonin is essential for the induction of cell-non-autonomous UPR^{mt} in response to neuronal Wnt signaling (Figure 7M). Ultimately, our study provides strong evidence that retromer-dependent Wnt signaling regulates the induction of the UPR^{mt} in the peripheral tissues, suggests that Wnt signaling regulates proteostasis, and indicates that Wnt pathway components should thus be viewed as therapeutic targets for age-related neurodegenerative diseases.

STAR★METHODS

Detailed methods are provided in the online version of this paper and include the following:

- KEY RESOURCES TABLE
- CONTACT FOR REAGENT AND RESOURCE SHARING
- EXPERIMENTAL MODEL AND SUBJECT DETAILS
 - *Caenorhabditis elegans* Maintenance and Transgenic Lines
- METHOD DETAILS
 - RNAi Feeding
 - Heat shock assay
 - ER stress assay
 - Analysis of the fluorescence intensity in whole worm
 - Western Blot Analysis
 - Antibodies
 - RNA Isolation and quantitative PCR analyses
 - Feed serotonin (5-HT)
 - Lifespan Analysis
- QUANTIFICATION AND STATISTICAL ANALYSIS

SUPPLEMENTAL INFORMATION

Supplemental Information includes seven figures and two tables and can be found with this article online at <https://doi.org/10.1016/j.cell.2018.06.029>.

ACKNOWLEDGMENTS

We thank Tian lab members for assistance with strain maintenance and reporter crosses. Several *C. elegans* strains used in this work were provided by *Caenorhabditis* Genetics Center (CGC), which is supported by the NIH-Officer of Research Infrastructure Programs (P40 OD010440) and the Japanese National BioResource Project. The DRP-1 construct was kindly provided by Dr. Chonglin Yang’s lab. Y.T. was supported by the National Key R&D Program of China (2017YFA0506400), the Strategic Priority Research Program of the Chinese Academy of Sciences (XDB13000000), and the National Natural Science Foundation of China (31771333). A.D. is supported by the Glenn Foundation for Medical Research, Howard Hughes Medical Institute (HHMI), and NIH (R01 ES021667 and R37 AG024365).

AUTHOR CONTRIBUTIONS

Y.T. and A.D. conceived the study and wrote the manuscript. Y.T. performed the EMS screen and isolated the mutants in A.D.’s lab. Q.Z., X.W., and P.C.

performed the *C. elegans* crosses, strain generation, RNAi experiments, and the fluorescence microscopy. Q.Z. and X.W. performed the qPCR experiments and the western blotting of *C. elegans*. Q.Z. performed the lifespan experiments. X.W. and N.X. made the transgene constructs. L.L. performed the microinjection experiments.

DECLARATION OF INTERESTS

A.D. is a cofounder of Proteostasis Therapeutics, Inc. and Mitobridge, Inc. and declares no financial interest related to this work.

Received: December 5, 2017

Revised: April 18, 2018

Accepted: June 13, 2018

Published: July 26, 2018

REFERENCES

- Bänziger, C., Soldini, D., Schütt, C., Zipperlen, P., Hausmann, G., and Basler, K. (2006). Wntless, a conserved membrane protein dedicated to the secretion of Wnt proteins from signaling cells. *Cell* 125, 509–522.
- Belenkaya, T.Y., Wu, Y., Tang, X., Zhou, B., Cheng, L., Sharma, Y.V., Yan, D., Selva, E.M., and Lin, X. (2008). The retromer complex influences Wnt secretion by recycling wntless from endosomes to the trans-Golgi network. *Dev. Cell* 14, 120–131.
- Benedetti, C., Haynes, C.M., Yang, Y., Harding, H.P., and Ron, D. (2006). Ubiquitin-like protein 5 positively regulates chaperone gene expression in the mitochondrial unfolded protein response. *Genetics* 174, 229–239.
- Berendzen, K.M., Durieux, J., Shao, L.W., Tian, Y., Kim, H.E., Wolff, S., Liu, Y., and Dillin, A. (2016). Neuroendocrine coordination of mitochondrial stress signaling and proteostasis. *Cell* 166, 1553–1563.
- Bonifacino, J.S., and Rojas, R. (2006). Retrograde transport from endosomes to the trans-Golgi network. *Nat. Rev. Mol. Cell Biol.* 7, 568–579.
- Brignull, H.R., Moore, F.E., Tang, S.J., and Morimoto, R.I. (2006). Polyglutamine proteins at the pathogenic threshold display neuron-specific aggregation in a pan-neuronal *Caenorhabditis elegans* model. *J. Neurosci.* 26, 7597–7606.
- Cai, H., Cong, W., Ji, S., Rothman, S., Maudsley, S., and Martin, B. (2012). Metabolic dysfunction in Alzheimer’s disease and related neurodegenerative disorders. *Curr. Alzheimer Res.* 9, 5–17.
- Chase, D.L., and Koelle, M.R. (2007). Biogenic amine neurotransmitters in *C. elegans*. *WormBook*, 1–15.
- Chen, D., Xiao, H., Zhang, K., Wang, B., Gao, Z., Jian, Y., Qi, X., Sun, J., Miao, L., and Yang, C. (2010). Retromer is required for apoptotic cell clearance by phagocytic receptor recycling. *Science* 327, 1261–1264.
- Chun, L., Gong, J., Yuan, F., Zhang, B., Liu, H., Zheng, T., Yu, T., Xu, X.Z.S., and Liu, J. (2015). Metabotropic GABA signalling modulates longevity in *C. elegans*. *Nat. Commun.* 6, 8828.
- Clevers, H. (2006). Wnt/beta-catenin signaling in development and disease. *Cell* 127, 469–480.
- Clevers, H., and Nusse, R. (2012). Wnt/β-catenin signaling and disease. *Cell* 149, 1192–1205.
- Coudreuse, D.Y.M., Roël, G., Betist, M.C., Destrée, O., and Korswagen, H.C. (2006). Wnt gradient formation requires retromer function in Wnt-producing cells. *Science* 312, 921–924.
- Dillin, A., Hsu, A.L., Arantes-Oliveira, N., Lehrer-Graiwer, J., Hsin, H., Fraser, A.G., Kamath, R.S., Ahringer, J., and Kenyon, C. (2002). Rates of behavior and aging specified by mitochondrial function during development. *Science* 298, 2398–2401.
- Douglas, P.M., Baird, N.A., Simic, M.S., Uhlein, S., McCormick, M.A., Wolff, S.C., Kennedy, B.K., and Dillin, A. (2015). Heterotypic signals from neural HSF-1 separate thermotolerance from longevity. *Cell Rep.* 12, 1196–1204.

- Dreier, L., Burbea, M., and Kaplan, J.M. (2005). LIN-23-mediated degradation of beta-catenin regulates the abundance of GLR-1 glutamate receptors in the ventral nerve cord of *C. elegans*. *Neuron* *46*, 51–64.
- Duarte, J.M.N., Schuck, P.F., Wenk, G.L., and Ferreira, G.C. (2013). Metabolic disturbances in diseases with neurological involvement. *Aging Dis.* *5*, 238–255.
- Durieux, J., Wolff, S., and Dillin, A. (2011). The cell-non-autonomous nature of electron transport chain-mediated longevity. *Cell* *144*, 79–91.
- Gleason, J.E., Szyleyko, E.A., and Eisenmann, D.M. (2006). Multiple redundant Wnt signaling components function in two processes during *C. elegans* vulval development. *Dev. Biol.* *298*, 442–457.
- Gleason, R.J., Akintobi, A.M., Grant, B.D., and Padgett, R.W. (2014). BMP signaling requires retromer-dependent recycling of the type I receptor. *Proc. Natl. Acad. Sci. USA* *111*, 2578–2583.
- Gorrepati, L., Krause, M.W., Chen, W., Brodigan, T.M., Correa-Mendez, M., and Eisenmann, D.M. (2015). Identification of Wnt pathway target genes regulating the division and differentiation of larval seam cells and vulval precursor cells in *Caenorhabditis elegans*. *G3 (Bethesda)* *5*, 1551–1566.
- Hardin, J., and King, R.S. (2008). The long and the short of Wnt signaling in *C. elegans*. *Curr. Opin. Genet. Dev.* *18*, 362–367.
- Haynes, C.M., Petrova, K., Benedetti, C., Yang, Y., and Ron, D. (2007). ClpP mediates activation of a mitochondrial unfolded protein response in *C. elegans*. *Dev. Cell* *13*, 467–480.
- Herman, M.A., Vassilieva, L.L., Horvitz, H.R., Shaw, J.E., and Herman, R.K. (1995). The *C. elegans* gene *lin-44*, which controls the polarity of certain asymmetric cell divisions, encodes a Wnt protein and acts cell nonautonomously. *Cell* *83*, 101–110.
- Hierro, A., Rojas, A.L., Rojas, R., Murthy, N., Effantin, G., Kajava, A.V., Steven, A.C., Bonifacino, J.S., and Hurley, J.H. (2007). Functional architecture of the retromer cargo-recognition complex. *Nature* *449*, 1063–1067.
- Higuchi-Sanabria, R., Frankino, P.A., Paul, J.W., 3rd, Tronnes, S.U., and Dillin, A. (2018). A futile battle? Protein quality control and the stress of aging. *Dev. Cell* *44*, 139–163.
- Houtkooper, R.H., Mouchiroud, L., Ryu, D., Moullan, N., Katsyuba, E., Knott, G., Williams, R.W., and Auwerx, J. (2013). Mitonuclear protein imbalance as a conserved longevity mechanism. *Nature* *497*, 451–457.
- Inestrosa, N.C., and Arenas, E. (2010). Emerging roles of Wnts in the adult nervous system. *Nat. Rev. Neurosci.* *11*, 77–86.
- Jackson, B.M., Abete-Luzi, P., Krause, M.W., and Eisenmann, D.M. (2014). Use of an activated beta-catenin to identify Wnt pathway target genes in *Caenorhabditis elegans*, including a subset of collagen genes expressed in late larval development. *G3 (Bethesda)* *4*, 733–747.
- Janda, C.Y., Waghray, D., Levin, A.M., Thomas, C., and Garcia, K.C. (2012). Structural basis of Wnt recognition by Frizzled. *Science* *337*, 59–64.
- Komiya, Y., and Habas, R. (2008). Wnt signal transduction pathways. *Organogenesis* *4*, 68–75.
- Korswagen, H.C., Coudreuse, D.Y.M., Betist, M.C., van de Water, S., Zivkovic, D., and Clevers, H.C. (2002). The Axin-like protein PRY-1 is a negative regulator of a canonical Wnt pathway in *C. elegans*. *Genes Dev.* *16*, 1291–1302.
- Labbadia, J., and Morimoto, R.I. (2015). The biology of proteostasis in aging and disease. *Annu. Rev. Biochem.* *84*, 435–464.
- Labrousse, A.M., Zappaterra, M.D., Rube, D.A., and van der Bliek, A.M. (1999). *C. elegans* dynamin-related protein DRP-1 controls severing of the mitochondrial outer membrane. *Mol. Cell* *4*, 815–826.
- Link, C.D., Cypser, J.R., Johnson, C.J., and Johnson, T.E. (1999). Direct observation of stress response in *Caenorhabditis elegans* using a reporter transgene. *Cell Stress Chaperones* *4*, 235–242.
- Logan, C.Y., and Nusse, R. (2004). The Wnt signaling pathway in development and disease. *Annu. Rev. Cell Dev. Biol.* *20*, 781–810.
- Malooof, J.N., Whangbo, J., Harris, J.M., Jongeward, G.D., and Kenyon, C. (1999). A Wnt signaling pathway controls *hox* gene expression and neuroblast migration in *C. elegans*. *Development* *126*, 37–49.
- Merkwirth, C., Jovaisaite, V., Durieux, J., Matilainen, O., Jordan, S.D., Quiros, P.M., Steffen, K.K., Williams, E.G., Mouchiroud, L., Tronnes, S.U., et al. (2016). Two conserved histone demethylases regulate mitochondrial stress-induced longevity. *Cell* *165*, 1209–1223.
- Morley, J.F., Brignull, H.R., Weyers, J.J., and Morimoto, R.I. (2002). The threshold for polyglutamine-expansion protein aggregation and cellular toxicity is dynamic and influenced by aging in *Caenorhabditis elegans*. *Proc. Natl. Acad. Sci. USA* *99*, 10417–10422.
- Nargund, A.M., Pellegrino, M.W., Fiorese, C.J., Baker, B.M., and Haynes, C.M. (2012). Mitochondrial import efficiency of ATFS-1 regulates mitochondrial UPR activation. *Science* *337*, 587–590.
- Nargund, A.M., Fiorese, C.J., Pellegrino, M.W., Deng, P., and Haynes, C.M. (2015). Mitochondrial and nuclear accumulation of the transcription factor ATFS-1 promotes OXPHOS recovery during the UPR(mt). *Mol. Cell* *58*, 123–133.
- Nusse, R., and Clevers, H. (2017). Wnt/ β -catenin signaling, disease, and emerging therapeutic modalities. *Cell* *169*, 985–999.
- Owusu-Ansah, E., Song, W., and Perrimon, N. (2013). Muscle mitohormesis promotes longevity via systemic repression of insulin signaling. *Cell* *155*, 699–712.
- Pan, C.L., Baum, P.D., Gu, M., Jorgensen, E.M., Clark, S.G., and Garriga, G. (2008). *C. elegans* AP-2 and retromer control Wnt signaling by regulating mig-14/Wntless. *Dev. Cell* *14*, 132–139.
- Reya, T., and Clevers, H. (2005). Wnt signalling in stem cells and cancer. *Nature* *434*, 843–850.
- Rocheleau, C.E., Downs, W.D., Lin, R., Wittmann, C., Bei, Y., Cha, Y.-H., Ali, M., Priess, J.R., and Mello, C.C. (1997). Wnt signaling and an APC-related gene specify endoderm in early *C. elegans* embryos. *Cell* *90*, 707–716.
- Ron, D., and Walter, P. (2007). Signal integration in the endoplasmic reticulum unfolded protein response. *Nat. Rev. Mol. Cell Biol.* *8*, 519–529.
- Ruvkun, G., and Hobert, O. (1998). The taxonomy of developmental control in *Caenorhabditis elegans*. *Science* *282*, 2033–2041.
- Sawa, H., Lobel, L., and Horvitz, H.R. (1996). The *Caenorhabditis elegans* gene *lin-17*, which is required for certain asymmetric cell divisions, encodes a putative seven-transmembrane protein similar to the *Drosophila* frizzled protein. *Genes Dev.* *10*, 2189–2197.
- Shackelford, G.M., Shivakumar, S., Shiue, L., Mason, J., Kenyon, C., and Varmus, H.E. (1993). Two wnt genes in *Caenorhabditis elegans*. *Oncogene* *8*, 1857–1864.
- Suomalainen, A., Elo, J.M., Pietiläinen, K.H., Hakonen, A.H., Sevastianova, K., Korpela, M., Isohanni, P., Marjavaara, S.K., Tyni, T., Kiuru-Enari, S., et al. (2011). FGF-21 as a biomarker for muscle-manifesting mitochondrial respiratory chain deficiencies: a diagnostic study. *Lancet Neurol.* *10*, 806–818.
- Taylor, R.C., and Dillin, A. (2013). XBP-1 is a cell-nonautonomous regulator of stress resistance and longevity. *Cell* *153*, 1435–1447.
- Thorpe, C.J., Schlesinger, A., Carter, J.C., and Bowerman, B. (1997). Wnt signaling polarizes an early *C. elegans* blastomere to distinguish endoderm from mesoderm. *Cell* *90*, 695–705.
- Tian, Y., Garcia, G., Bian, Q., Steffen, K.K., Joe, L., Wolff, S., Meyer, B.J., and Dillin, A. (2016). Mitochondrial stress induces chromatin reorganization to promote longevity and UPR(mt). *Cell* *165*, 1197–1208.
- Wang, S., and Bellen, H.J. (2015). The retromer complex in development and disease. *Development* *142*, 2392–2396.
- Wang, W., Wang, X., Fujioka, H., Hoppel, C., Whone, A.L., Caldwell, M.A., Cullen, P.J., Liu, J., and Zhu, X. (2016). Parkinson's disease-associated mutant VPS35 causes mitochondrial dysfunction by recycling DLP1 complexes. *Nat. Med.* *22*, 54–63.

- Whangbo, J., and Kenyon, C. (1999). A Wnt signaling system that specifies two patterns of cell migration in *C. elegans*. *Mol. Cell* 4, 851–858.
- Wodarz, A., and Nusse, R. (1998). Mechanisms of Wnt signaling in development. *Annu. Rev. Cell Dev. Biol.* 14, 59–88.
- Yang, P.T., Lorenowicz, M.J., Silhankova, M., Coudreuse, D.Y.M., Betist, M.C., and Korswagen, H.C. (2008). Wnt signaling requires retromer-dependent recycling of MIG-14/Wntless in Wnt-producing cells. *Dev. Cell* 14, 140–147.
- Yoon, J.C., Ng, A., Kim, B.H., Bianco, A., Xavier, R.J., and Elledge, S.J. (2010). Wnt signaling regulates mitochondrial physiology and insulin sensitivity. *Genes Dev.* 24, 1507–1518.
- Zhang, D., Isack, N.R., Glodowski, D.R., Liu, J., Chen, C.C.-H., Xu, X.Z.S., Grant, B.D., and Rongo, C. (2012). RAB-6.2 and the retromer regulate glutamate receptor recycling through a retrograde pathway. *J. Cell Biol.* 196, 85–101.

STAR★METHODS

KEY RESOURCES TABLE

REAGENT or RESOURCE	SOURCE	IDENTIFIER
Antibodies		
Mouse monoclonal anti-GFP (B-2)	Santa Cruz Biotechnology	Cat#sc-9996; RRID: AB_627695
Mouse monoclonal anti-Tubulin (B-5-1-2)	Sigma	Cat#T6074; RRID: AB_477582
Rabbit polyclonal anti-mCherry	Gene TEX	Cat#GTX128508
HRP-Goat anti-mouse IgG	EarthOx	Cat#E030110; RRID: AB_2572419
HRP-Goat anti-Rabbit IgG	EASYBIO	Cat#BE1010
Bacterial and Virus Strains		
OP50	CGC	N/A
HT115	CGC	N/A
DH5 α	Tiagen	Cat#CB101
Chemicals, Peptides, and Recombinant Proteins		
AGAROSE	Life Technology	Cat#202007
GeneGreen	Tiagen	Cat#RT210
Ethylenediamine tetraacetic acid	Sigma	Cat#E9884
Trizma base	Sigma	Cat#V900483
Sodium chloride	Sigma	Cat#V900058
Bacto Agar	BD	Cat#214010
Bacto Peptone	BD	Cat#211677
Cholesterol	Sigma	Cat#C8667
Calcium chloride dihydrate	Sigma	Cat#C7902
Magnesium sulfate heptahydrate	Sigma	Cat#M1880
Potassium phosphate monobasic	Sigma	Cat#V900041
Potassium phosphate dibasic	Sigma	Cat#V900050
Sodium phosphate dibasic	Sigma	Cat#V900061
Isopropyl beta-D-thiogalactoside	Sigma	Cat#V900917
Carbenicillin Na2	INALCO	Cat#1758-9317
TRYPTONE	OXOID	Cat#CM0129
YEAST EXTRACT	OXOID	Cat#LP0021
Potassium chloride	Sigma	Cat#V900068
Glycine	Amresco	Cat#0167
Tween 20	Sigma	Cat#P1379
TGX FastCast Acrylamide Kit, 10%	BIO-RAD	Cat#1610172
TEMED	Sigma	Cat#T22500
Ammonium persulfate	Sigma	Cat#V900883
Sodium dodecyl sulfate	Sigma	Cat#V900859
Trans buffer	BIO-RAD	Cat#10026938
TRIzol	Invitrogen	Cat#15596026
Sodium acetate buffer solution	Sigma	Cat#S7899
FUDR	Aladdin	Cat#F110732
5-HT hydrochloride powder	Sigma	Cat#H9523
Tunicamycin	Abcam	Cat#ab120296
Critical Commercial Assays		
Tanon High-sig ECL Western Blotting Substrate	Tanon	Cat#180-501
KOD-Plus-Neo	Toyobo Life Science Department	Cat#KOD-401

(Continued on next page)

Continued

REAGENT or RESOURCE	SOURCE	IDENTIFIER
M-MLV Reverse Transcriptase	Invitrogen	Cat#28025013
RQ1 RNase-Free DNase	Promega	Cat#M6101
RNasin Ribonuclease Inhibitor	Promega	Cat#N2111
iTaq Universal SYBR Green Supermix	BIO-RAD	Cat#1725121
One Step Cloning Kit	Vazyme	Cat#C112
2 x Taq Mix	Tiagen	Cat#KT201
KOD-Plus- Mutagenesis Kit	Toyobo Life Science Department	Cat#SMK-101
Experimental Models: Organisms/Strains		
<i>C. elegans</i> : Bristol (N2) strain as wild-type (WT)	CGC	N2
<i>C. elegans</i> : SJ4100 (zcls13[hsp-6p::gfp] V)	CGC	WormBase: SJ4100
<i>C. elegans</i> : AM101 (rmls110[rgef-1p::Q40::yfp])	CGC	WormBase: AM101
<i>C. elegans</i> : AGD785 (rmls110[rgef-1p::Q40::yfp]; zcls13[hsp-6p::gfp] V)	Tian et al., 2016	N/A
<i>C. elegans</i> : SJ4005 (zcls4[hsp-4p::gfp] V)	CGC	WormBase: SJ4005
<i>C. elegans</i> : CL2070 (dvls70[hsp-16.2p::gfp + rol-6(su1006)])	CGC	WormBase: CL2070
<i>C. elegans</i> : SJ4197 (zcls39[dve-1p::dve-1::gfp])	CGC	WormBase: SJ4197
<i>C. elegans</i> : VC1390 (vps-35(ok1880) II)	CGC	WormBase: VC1390
<i>C. elegans</i> : HC196 (sid-1(qt9) V)	CGC	WormBase: HC196
<i>C. elegans</i> : AGD927 (uths270[rab-3p::xbp-1 s + myo-2p::tdTomato])	CGC	WormBase: AGD927
<i>C. elegans</i> : uths368[rab-3p::hsf-1 + myo-2p::tdTomato]	This Study	N/A
<i>C. elegans</i> : CF1553 (muls84[sod-3p::gfp + rol-6(su1006)])	CGC	WormBase: CF1553
<i>C. elegans</i> : vps-26(tm1523) IV	National Bioresource Project, Tokyo, Japan	WormBase: WBVar00250513
<i>C. elegans</i> : vps-29(tm1320) III	National Bioresource Project, Tokyo, Japan	WormBase: WBVar00250318
<i>C. elegans</i> : EW12 (mig-14(ga62) II)	CGC	WormBase: EW12
<i>C. elegans</i> : CB840 (dpy-23(e840) X)	CGC	WormBase: CB840
<i>C. elegans</i> : KP4 (glr-1(n2461) III)	CGC	WormBase: KP4
<i>C. elegans</i> : CB3203 (ced-1(e1735) I)	CGC	WormBase: CB3203
<i>C. elegans</i> : LT186 (sma-6(wk-7) II)	CGC	WormBase: LT186
<i>C. elegans</i> : drp-1(tm1108) IV	National Bioresource Project, Tokyo, Japan	WormBase: WBVar00250125
<i>C. elegans</i> : MT1215 (egl-20(n585) IV)	CGC	WormBase: MT1215
<i>C. elegans</i> : RB763 (cwn-1(ok546) II)	CGC	WormBase: RB763
<i>C. elegans</i> : VC636 (cwn-2(ok895) IV)	CGC	WormBase: VC636
<i>C. elegans</i> : MT5383 (lin-44(n1792) I)	CGC	WormBase: MT5383
<i>C. elegans</i> : CB3303 (mig-1(e1787) I)	CGC	WormBase: CB3303
<i>C. elegans</i> : PS1403 (lin-17(sy277) I)	CGC	WormBase: PS1403
<i>C. elegans</i> : MT15434 (tph-1(mg280) II)	CGC	WormBase: MT15434
<i>C. elegans</i> : SJ4103 (zcls14[myo-3p::gfp(mit)])	CGC	WormBase: SJ4103
<i>C. elegans</i> : AQ866 (ser-4(ok512) III)	CGC	WormBase: AQ866
<i>C. elegans</i> : DA2100 (ser-7(tm1325) X)	CGC	WormBase: DA2100
<i>C. elegans</i> : MT301 (ser-1(ok345) X)	CGC	WormBase: MT301
<i>C. elegans</i> : DA2109 (ser-7(tm1325) X; ser-1(ok345) X)	CGC	WormBase: DA2109
<i>C. elegans</i> : MT9668 (mod-1(ok103) V)	CGC	WormBase: MT9668
<i>C. elegans</i> : AGD1001 (uth13; rmls110[rgef-1p::Q40::yfp]; zcls13[hsp-6p::gfp])	This Study	N/A

(Continued on next page)

Continued

REAGENT or RESOURCE	SOURCE	IDENTIFIER
<i>C. elegans</i> : AGD1619 (<i>vps-35(ok1880)</i> II; <i>rmls110[rgef-1p::Q40::yfp]</i> ; <i>zcls13[hsp-6p::gfp]</i>)	This Study	N/A
<i>C. elegans</i> : AGD1617(<i>vps-35(ok1880)</i> II; <i>zcls13[hsp-6p::gfp]</i>)	This Study	N/A
<i>C. elegans</i> : AGD1647 (<i>vps-35(ok1880)</i> II; <i>zcls4[hsp-4p::gfp]</i>)	This Study	N/A
<i>C. elegans</i> : AGD1648 (<i>vps-35(ok1880)</i> II; <i>dvls70[hsp-16.2p::gfp + rol-6(su1006)]</i>)	This Study	N/A
<i>C. elegans</i> : AGD1075 (<i>sid-1(qt9)</i> V; <i>zcls13[hsp-6p::gfp]</i> V; <i>uths375[unc-119p::cco-1 HP + rol-6(su1006)]</i>)	This Study	N/A
<i>C. elegans</i> : AGD1650 (<i>vps-35(ok1880)</i> II; <i>sid-1(qt9)</i> V; <i>zcls13[hsp-6p::gfp]</i> V; <i>uths375[unc-119p::cco-1 HP + rol-6(su1006)]</i>)	This Study	N/A
<i>C. elegans</i> : LTY243 (<i>egl-20(n585)</i> IV; <i>sid-1(qt9)</i> V; <i>zcls13[hsp-6p::gfp]</i> V; <i>uths375[unc-119p::cco-1 HP + rol-6(su1006)]</i>)	This Study	N/A
<i>C. elegans</i> : AGD928 (<i>uths270[rab-3p::xbp-1 s + myo-2p::tdTomato]</i> ; <i>zcls4[hsp-4p::gfp]</i>)	This Study	N/A
<i>C. elegans</i> : AGD1649 (<i>vps-35(ok1880)</i> II; <i>uths270[rab-3p::xbp-1 s + myo-2p::tdTomato]</i> ; <i>zcls4[hsp-4p::gfp]</i>)	This Study	N/A
<i>C. elegans</i> : AGD1199 (<i>uths368[rab-3p::hsf-1 + myo-2p::tdTomato]</i> ; <i>mls84[sod-3p::gfp]</i>)	This Study	N/A
<i>C. elegans</i> : LTY152 (<i>vps-35(ok1880)</i> II; <i>uths368[rab-3p::hsf-1 + myo-2p::tdTomato]</i> ; <i>mls84[sod-3p::gfp]</i>)	This Study	N/A
<i>C. elegans</i> : LTY1 (<i>vps-26(tm1523)</i> IV; <i>rmls110[rgef-1p::Q40::yfp]</i> ; <i>zcls13[hsp-6p::gfp]</i>)	This Study	N/A
<i>C. elegans</i> : LTY179 (<i>vps-29(tm1320)</i> III; <i>rmls110[rgef-1p::Q40::yfp]</i> ; <i>zcls13[hsp-6p::gfp]</i>)	This Study	N/A
<i>C. elegans</i> : AGD1638 (<i>mig-14(ga62)</i> II; <i>rmls110[rgef-1p::Q40::yfp]</i> ; <i>zcls13[hsp-6p::gfp]</i>)	This Study	N/A
<i>C. elegans</i> : AGD1639 (<i>dpy-23(e840)</i> X; <i>rmls110[rgef-1p::Q40::yfp]</i> ; <i>zcls13[hsp-6p::gfp]</i>)	This Study	N/A
<i>C. elegans</i> : LTY244 (<i>ythEx56[drp-1p::mCherry::drp-1 + myo-2p::tdTomato]</i> ; <i>zcls13[hsp-6p::gfp]</i>)	This Study	N/A
<i>C. elegans</i> : LTY245 (<i>ythEx56[drp-1p::mCherry::drp-1 + myo-2p::tdTomato]</i> ; <i>rmls110[rgef-1p::Q40::yfp]</i> ; <i>zcls13[hsp-6p::gfp]</i>)	This Study	N/A
<i>C. elegans</i> : LTY248 (<i>ythEx60[mig-14p::mig-14::mCherry + myo-2p::tdTomato]</i> ; <i>rmls110[rgef-1p::Q40::yfp]</i> ; <i>zcls13[hsp-6p::gfp]</i> ; <i>vps-35(ok1880)</i> II)	This Study	N/A
<i>C. elegans</i> : AGD1643 (<i>glr-1(n2461)</i> III; <i>rmls110[rgef-1p::Q40::yfp]</i> ; <i>zcls13[hsp-6p::gfp]</i>)	This Study	N/A
<i>C. elegans</i> : LTY166 (<i>ced-1(e1735)</i> I; <i>rmls110[rgef-1p::Q40::yfp]</i> ; <i>zcls13[hsp-6p::gfp]</i>)	This Study	N/A
<i>C. elegans</i> : LTY167 (<i>drp-1(tm1108)</i> IV; <i>rmls110[rgef-1p::Q40::yfp]</i> ; <i>zcls13[hsp-6p::gfp]</i>)	This Study	N/A
<i>C. elegans</i> : LTY4 (<i>sma-6(wk7)</i> II; <i>rmls110[rgef-1p::Q40::yfp]</i> ; <i>zcls13[hsp-6p::gfp]</i>)	This Study	N/A
<i>C. elegans</i> : AGD1620 (<i>egl-20(n585)</i> IV; <i>rmls110[rgef-1p::Q40::yfp]</i> ; <i>zcls13[hsp-6p::gfp]</i>)	This Study	N/A
<i>C. elegans</i> : AGD1644 (<i>egl-20(n585)</i> IV; <i>rmls110[rgef-1p::Q40::yfp]</i> ; <i>zcls39[dve-1p::dve-1::gfp]</i>)	This Study	N/A

(Continued on next page)

Continued

REAGENT or RESOURCE	SOURCE	IDENTIFIER
<i>C. elegans</i> : AGD1618 (<i>egl-20(n585)</i> IV; <i>zcls13</i> [<i>hsp-6p::gfp</i>])	This Study	N/A
<i>C. elegans</i> : AGD1641 (<i>cwn-1(ok546)</i> II; <i>rmls110</i> [<i>rgef-1p::Q40::yfp</i>]; <i>zcls13</i> [<i>hsp-6p::gfp</i>])	This Study	N/A
<i>C. elegans</i> : LTY90 (<i>cwn-2(ok895)</i> IV; <i>rmls110</i> [<i>rgef-1p::Q40::yfp</i>]; <i>zcls13</i> [<i>hsp-6p::gfp</i>])	This Study	N/A
<i>C. elegans</i> : AGD1640 (<i>lin-44(n1792)</i> I; <i>rmls110</i> [<i>rgef-1p::Q40::yfp</i>]; <i>zcls13</i> [<i>hsp-6p::gfp</i>])	This Study	N/A
<i>C. elegans</i> : LTY56 (<i>ythls6</i> [<i>egl-20p::mCherry + rol-6</i>])	This Study	N/A
<i>C. elegans</i> : LTY61 (<i>rmls110</i> [<i>rgef-1p::Q40::yfp</i>]; <i>ythls6</i> [<i>egl-20p::mCherry + rol-6</i>])	This Study	N/A
<i>C. elegans</i> : LTY59 (<i>ythls8</i> [<i>egl-20p::egl-20::mCherry + rol-6</i>])	This Study	N/A
<i>C. elegans</i> : LTY11 (<i>ythEx4</i> [<i>egl-20p::egl-20::mCherry + rol-6</i>])	This Study	N/A
<i>C. elegans</i> : LTY155 (<i>rmls110</i> [<i>rgef-1p::Q40::yfp</i>]; <i>ythls8</i> [<i>egl-20p::egl-20::mCherry + rol-6</i>])	This Study	N/A
<i>C. elegans</i> : LTY195 (<i>vps-35(ok1880)</i> II; <i>ythEx4</i> [<i>egl-20p::egl-20::mCherry + rol-6</i>])	This Study	N/A
<i>C. elegans</i> : LTY68 (<i>mig-14(ga62)</i> II; <i>ythEx4</i> [<i>egl-20p::egl-20::mCherry + rol-6</i>])	This Study	N/A
<i>C. elegans</i> : LTY2 (<i>mig-1(e1787)</i> I; <i>rmls110</i> [<i>rgef-1p::Q40::yfp</i>]; <i>zcls13</i> [<i>hsp-6p::gfp</i>])	This Study	N/A
<i>C. elegans</i> : LTY180 (<i>lin-17(sy277)</i> I; <i>rmls110</i> [<i>rgef-1p::Q40::yfp</i>]; <i>zcls13</i> [<i>hsp-6p::gfp</i>])	This Study	N/A
<i>C. elegans</i> : LTY92 (<i>mig-1(e1787)</i> I; <i>zcls13</i> [<i>hsp-6p::gfp</i>])	This Study	N/A
<i>C. elegans</i> : LTY24 (<i>ythls1</i> [<i>gly-19p::egl-20 + myo-2p::tdTomato</i>])	This Study	N/A
<i>C. elegans</i> : LTY25 (<i>ythls2</i> [<i>gly-19p::egl-20 + myo-2p::tdTomato</i>])	This Study	N/A
<i>C. elegans</i> : LTY26 (<i>ythls3</i> [<i>rgef-1p::egl-20 + myo-2p::tdTomato</i>])	This Study	N/A
<i>C. elegans</i> : LTY27 (<i>ythls4</i> [<i>rgef-1p::egl-20 + myo-2p::tdTomato</i>])	This Study	N/A
<i>C. elegans</i> : LTY37 (<i>ythls1</i> [<i>gly-19p::egl-20 + myo-2p::tdTomato</i>]; <i>zcls39</i> [<i>dve-1p::dve-1::gfp</i>])	This Study	N/A
<i>C. elegans</i> : LTY38 (<i>ythls2</i> [<i>gly-19p::egl-20 + myo-2p::tdTomato</i>]; <i>zcls39</i> [<i>dve-1p::dve-1::gfp</i>])	This Study	N/A
<i>C. elegans</i> : LTY39 (<i>ythls3</i> [<i>rgef-1p::egl-20 + myo-2p::tdTomato</i>]; <i>zcls39</i> [<i>dve-1p::dve-1::gfp</i>])	This Study	N/A
<i>C. elegans</i> : LTY40 (<i>ythls4</i> [<i>rgef-1p::egl-20 + myo-2p::tdTomato</i>]; <i>zcls39</i> [<i>dve-1p::dve-1::gfp</i>])	This Study	N/A
<i>C. elegans</i> : LTY41 (<i>ythls1</i> [<i>gly-19p::egl-20 + myo-2p::tdTomato</i>]; <i>zcls13</i> [<i>hsp-6p::gfp</i>])	This Study	N/A
<i>C. elegans</i> : LTY42 (<i>ythls2</i> [<i>gly-19p::egl-20 + myo-2p::tdTomato</i>]; <i>zcls13</i> [<i>hsp-6p::gfp</i>])	This Study	N/A
<i>C. elegans</i> : LTY43 (<i>ythls3</i> [<i>rgef-1p::egl-20 + myo-2p::tdTomato</i>]; <i>zcls13</i> [<i>hsp-6p::gfp</i>])	This Study	N/A
<i>C. elegans</i> : LTY44 (<i>ythls4</i> [<i>rgef-1p::egl-20 + myo-2p::tdTomato</i>]; <i>zcls13</i> [<i>hsp-6p::gfp</i>])	This Study	N/A
<i>C. elegans</i> : LTY181 (<i>ythEx41</i> [<i>myo-2p::egl-20::mCherry + rol-6</i>]; <i>zcls13</i> [<i>hsp-6p::gfp</i>])	This Study	N/A

(Continued on next page)

Continued

REAGENT or RESOURCE	SOURCE	IDENTIFIER
<i>C. elegans</i> : LTY177 (ythEx39[myo-3p::egl-20::mCherry + rol-6]; zcls13[hsp-6p::gfp])	This Study	N/A
<i>C. elegans</i> : LTY198 (ythEx44[lin-26p::egl-20::mCherry + rol-6]; zcls13[hsp-6p::gfp])	This Study	N/A
<i>C. elegans</i> : LTY139 (ythls3[rgef-1p::egl-20 + myo-2p::tdTomato]; zcls4[hsp-4p::gfp])	This Study	N/A
<i>C. elegans</i> : LTY137 (ythls1[gly-19p::egl-20 + myo-2p::tdTomato]; zcls4[hsp-4p::gfp])	This Study	N/A
<i>C. elegans</i> : LTY138 (ythls3[rgef-1p::egl-20 + myo-2p::tdTomato]; dvlS70[hsp-16.2p::gfp + rol-6(su1006)])	This Study	N/A
<i>C. elegans</i> : LTY136 (ythls1[gly-19p::egl-20 + myo-2p::tdTomato]; dvlS70[hsp-16.2p::gfp + rol-6(su1006)])	This Study	N/A
<i>C. elegans</i> : LTY206 (ythls3[rgef-1p::egl-20 + myo-2p::tdTomato]; zcls14[myo-3p::gfp(mit)])	This Study	N/A
<i>C. elegans</i> : LTY208 (ythls1[gly-19p::egl-20 + myo-2p::tdTomato]; zcls14[myo-3p::gfp(mit)])	This Study	N/A
<i>C. elegans</i> : LTY151 (ythls8[egl-20p::egl-20::mCherry + rol-6]; zcls13[hsp-6p::gfp])	This Study	N/A
<i>C. elegans</i> : LTY81 (vps-35(ok1880) II; ythls1[gly-19p::egl-20 + myo-2p::tdTomato]; zcls13[hsp-6p::gfp])	This Study	N/A
<i>C. elegans</i> : LTY79 (tph-1(mg280) II; ythls1[gly-19p::egl-20 + myo-2p::tdTomato]; zcls13[hsp-6p::gfp])	This Study	N/A
<i>C. elegans</i> : LTY78 (vps-35(ok1880) II; ythls3[rgef-1p::egl-20 + myo-2p::tdTomato]; zcls13[hsp-6p::gfp])	This Study	N/A
<i>C. elegans</i> : LTY72 (tph-1(mg280) II; ythls3[rgef-1p::egl-20 + myo-2p::tdTomato]; zcls13[hsp-6p::gfp])	This Study	N/A
<i>C. elegans</i> : LTY109 (ythEx22[egl-20p::vps-35 + myo-2p::tdTomato]; vps-35(ok1880) II; rmls110[rgef-1p::Q40::yfp]; zcls13[hsp-6p::gfp])	This Study	N/A
<i>C. elegans</i> : LTY183 (ythEx43[gly-19p::vps-35 + myo-2p::tdTomato]; vps-35(ok1880) II; rmls110[rgef-1p::Q40::yfp]; zcls13[hsp-6p::gfp])	This Study	N/A
<i>C. elegans</i> : LTY238 (ythEx51[rgef-1p::vps-35 + myo-2p::tdTomato]; vps-35(ok1880) II; rmls110[rgef-1p::Q40::yfp]; zcls13[hsp-6p::gfp])	This Study	N/A
<i>C. elegans</i> : LTY120 (ythEx33[tph-1p::egl-20::mCherry + rol-6]; zcls13[hsp-6p::gfp])	This Study	N/A
<i>C. elegans</i> : LTY164 (ser-4(ok512) III; ythls3[rgef-1p::egl-20 + myo-2p::tdTomato]; zcls13[hsp-6p::gfp])	This Study	N/A
<i>C. elegans</i> : LTY165 (ser-7(tm1325) X; ythls3[rgef-1p::egl-20 + myo-2p::tdTomato]; zcls13[hsp-6p::gfp])	This Study	N/A
<i>C. elegans</i> : LTY163 (ser-1(ok345) X; ythls3[rgef-1p::egl-20 + myo-2p::tdTomato]; zcls13[hsp-6p::gfp])	This Study	N/A
<i>C. elegans</i> : LTY199 (ser-7(tm1325) X; ser-1(ok345) X; ythls3[rgef-1p::egl-20 + myo-2p::tdTomato]; zcls13[hsp-6p::gfp])	This Study	N/A
<i>C. elegans</i> : LTY204 (mod-1(ok103) V; ythls3[rgef-1p::egl-20 + myo-2p::tdTomato]; zcls39[dve-1p::dve-1::gfp])	This Study	N/A
<i>C. elegans</i> : LTY169 (ythEx35[rgef-1p::egl-20N::mCherry + rol-6]; zcls13[hsp-6p::gfp])	This Study	N/A
<i>C. elegans</i> : LTY170 (ythEx36[rgef-1p::egl-20C::mCherry + rol-6]; zcls13[hsp-6p::gfp])	This Study	N/A

(Continued on next page)

Continued

REAGENT or RESOURCE	SOURCE	IDENTIFIER
<i>C. elegans</i> : LTY155 (ythIs8[egl-20p::egl-20::mCherry + rol-6]; ythEx47[rgef-1p::yfp])	This Study	N/A
Oligonucleotides		
See Table S2 for primer sequences	N/A	N/A
Recombinant DNA		
<i>egl-20p::egl-20::mCherry</i>	This Study	N/A
<i>rgef-1p::egl-20::mCherry</i>	This Study	N/A
<i>gly-19p::egl-20::mCherry</i>	This Study	N/A
<i>rgef-1p::egl-20</i>	This Study	N/A
<i>gly-19p::egl-20</i>	This Study	N/A
<i>egl-20p::mCherry</i>	This Study	N/A
<i>egl-20p::vps-35</i>	This Study	N/A
<i>rgef-1p::vps-35</i>	This Study	N/A
<i>gly-19p::vps-35</i>	This Study	N/A
<i>tph-1p::egl-20::mCherry</i>	This Study	N/A
<i>myo-3p::egl-20::mCherry</i>	This Study	N/A
<i>myo-2p::egl-20::mCherry</i>	This Study	N/A
<i>lin-26p::egl-20::mCherry</i>	This Study	N/A
<i>rgef-1p::egl-20N::mCherry</i>	This Study	N/A
<i>rgef-1p::egl-20C::mCherry</i>	This Study	N/A
<i>mig-14p::mig-14::mCherry</i>	This Study	N/A
<i>drp-1p::mCherry::drp-1</i>	Dr. Chonglin Yang lab	N/A
<i>rgef-1p::yfp</i>	This Study	N/A
Software and Algorithms		
GraphPad Prism 5	GraphPad Software	https://www.graphpad.com/scientificsoftware/prism/
Excel 2013	Microsoft	https://products.office.com/en-us/excel
ImageJ 1.48v	Wayne Rasband (NIH)	https://imagej.nih.gov/ij/
Zen	Zeiss	https://www.zeiss.com/microscopy/us/products/microscope-software/zen.html

CONTACT FOR REAGENT AND RESOURCE SHARING

Further information and requests for reagents maybe directed to and will be fulfilled by Andrew Dillin (dillin@berkeley.edu).

EXPERIMENTAL MODEL AND SUBJECT DETAILS

Carenorhabditis elegans Maintenance and Transgenic Lines

The following strains used in this study were obtained from the Caenorhabditis Genome Center (Minneapolis, MN): Bristol (N2) strain as wild-type (WT) strain, SJ4100 (zcls13[hsp-6p::gfp] V), AM101 (rmls110[rgef-1p::Q40::yfp]), SJ4005 (zcls4[hsp-4p::gfp] V), CL2070 (dvlS70[hsp-16.2p::gfp + rol-6(su1006)]), SJ4197 (zcls39[dve-1p::dve-1::gfp]), VC1390 (vps-35(ok1880) II), EW12 (mig-14(ga62) II), CB40 (dpy-23(e840) X), KP4 (glr-1(n2461) III), CB3203 (ced-1(e1735) I), MT1215 (egl-20(n585) IV), RB763 (cwn-1(ok546) II), VC636 (cwn-2(ok895) IV), MT5383 (lin-44(n1792) I), CB3303 (mig-1(e1787) I), PS1403 (lin-17(sy277) I), MT15434 (tph-1(mg280) II).

The following strains used in this study were obtained from the the National BioResource Project (Tokyo, Japan): vps-26(tm1523) IV, vps-29(tm1320) III, drp-1(tm1108) IV.

The following strains used in this study were generated in our lab: ythIs6[egl-20p::mCherry + rol-6], ythIs8[egl-20p::egl-20::mCherry + rol-6], ythIs1[gly-19p::egl-20 + myo-2p::tdTomato], ythIs2[gly-19p::egl-20 + myo-2p::tdTomato], ythIs3[rgef-1p::egl-20+myo-2p::tdTomato], ythIs4[rgef-1p::egl-20+myo-2p::tdTomato], ythEx4[egl-20p::egl-20::mCherry+rol-6], ythEx47 [rgef-1p::yfp], LTY109 (ythEx22[egl-20p::vps-35 + myo-2p::tdTomato]; vps-35(ok1880) II; rmls110[rgef-1p::Q40::yfp]; zcls13 [hsp-6p::gfp]), LTY183 (ythEx43[gly-19p::vps-35+myo-2p::tdTomato]; vps-35(ok1880); rmls110[rgef-1p::Q40::yfp]; zcls13

[*hsp-6p::gfp*], LTY238 (*ythEx51[rgef-1p::vps-35+myo-2p::tdTomato]; vps-35(ok1880); rmls110[rgef-1p::Q40::yfp]; zcls13[hsp-6p::gfp]*), LTY181 (*ythEx43[myo-2p::egl-20::mCherry+rol-6]; zcls13[hsp-6p::gfp]*), LTY177 (*ythEx39[myo-3p::egl-20::mCherry+rol-6]; zcls13[hsp-6p::gfp]*), LTY120 (*ythEx33[tph-1p::egl-20::mCherry+rol-6]; zcls13[hsp-6p::gfp]*), LTY114 (*ythEx27[tph-1p::egl-20::mCherry+rol-6]; zcls39[dve-1p::dve-1::gfp]*), LTY195 (*ythEx44[lin-26p::egl-20::mCherry+rol-6]; zcls13[hsp-6p::gfp]*), LTY169 (*ythEx35[rgef-1p::egl-20N::mCherry+rol-6]; zcls13[hsp-6p::gfp]*), LTY170 (*ythEx36[rgef-1p::egl-20C::mCherry+rol-6]; zcls13[hsp-6p::gfp]*), LTY110 (*ythEx23[rgef-1p::egl-20::mCherry+rol-6]; zcls39[dve-1p::dve-1::gfp]*), LTY118 (*ythEx31[gly-19p::egl-20::mCherry+rol-6]; zcls39[dve-1p::dve-1::gfp]*), LTY135 (*ythEx34[rgef-1p::egl-20::mCherry+rol-6]; zcls13[hsp-6p::gfp]; egl-20(n585) IV*), LTY245 (*ythEx56[drp-1p::mCherry::drp-1 + myo-2p::tdTomato]; rmls110[rgef-1p::Q40::yfp]; zcls13[hsp-6p::gfp]*), LTY248 (*ythEx60[mig-14p::mig-14::mCherry+myo-2p::tdTomato]; zcls13[hsp-6p::gfp]; vps-35(ok1880)*).

Nematodes were maintained and experimentally examined at 20°C on standard nematode growth medium agar plates seeded with *Escherichia coli* OP50.

For generation of *egl-20p::mCherry* strain, the *egl-20* 1.8 kb promoter was PCR amplified from genomic DNA and cloned into pNB23(*sur-5p::mCherry*) using SphI and XmaI. For the *egl-20p::egl-20::mCherry* strain, the *egl-20* cDNA (1179 bp) without stop codon was inserted into *egl-20p::mCherry* construct with XmaI and XbaI. To replace *egl-20* promoter, the *rgef-1*, *gly-19*, *lin-26*, *myo-2*, *myo-3* and *tph-1* promoter was cloned in place of the *egl-20* promoter in the *egl-20p::egl-20::mCherry* plasmid. To replace *egl-20* cDNA with half of *egl-20*, we use KOD-plus-Mutagenesis Kit to generate *egl-20N* (720bp) and *egl-20C* (462bp) plasmid.

Transgenic strains were generated by microinjecting target constructs (50ng/ul) mixed with a pRF4(*rol-6*) (50ng/ul) or a *myo-2p::tdTomato* (25ng/ul) co-injection maker. Integrated lines were generated using UV irradiation and backcrossed six times.

METHOD DETAILS

RNAi Feeding

Age synchronized worms were bleached and grown from hatch on *Escherichia coli* HT115 strains containing an empty vector control or double-stranded RNA. RNAi strains were from the Vidal library if present, or the Ahringer library if absent from the Vidal library.

Heat shock assay

Synchronized Day 1 adult worms of different genetic backgrounds grown on solid NGM plates were incubated in 34°C for 20 minutes.

ER stress assay

Synchronized L4 stage worms of different genetic backgrounds were incubate in M9 buffer containing 25 ng/μl tunicamycin or equivalent DMSO for 4 hours.

Analysis of the fluorescence intensity in whole worm

For whole-animal fluorescence image, worms were anesthetized with 50mM sodium azide, and imaged using a Leica M165 FC dissecting microscope. To quantify GFP fluorescence, the entire intestine regions were outlined and quantified using ImageJ software. For quantifying the localization of DVE-1::GFP fusion reporter, worms were mounted on 2% agarose pads with 50Mm and photographs were taken using a Zeiss Imager M2 microscope. Confocal images were taken using Zeiss LSM700.

Western Blot Analysis

Worms were synchronized and collected for western blot analysis. 100-150 worms were picked into 16μl M9 buffer and frozen in liquid nitrogen and kept at -80 until all the samples are ready for analysis. Before running the western blot gels, 5 x SDS loading buffer were added to each sample, mixed well and boiled for 15 min and resolved by Bio-Rad gels.

Antibodies

Antibodies used for western blot analysis were as follows: anti-GFP antibody (Santa Cruz Biotechnology sc-9996); anti-Tubulin antibody (Sigma T6074); anti-mCherry (GTX128508), anti-mouse secondary antibody (EarthOx E030110); anti-rabbit secondary antibody (EASYBIO BE1010).

RNA Isolation and quantitative PCR analyses

Total RNA was isolated using TRIzol (Invitrogen). Worms were synchronized and washed off the plates using M9 buffer, and 500 ul TRIzol were added to the samples and homogenized by repeated freezing and thawing using liquid nitrogen. RNA was isolated according to manufacturer's instructions. DNA was wiped off using RQ1 RNase-Free DNase (Promega). cDNA was synthesized using the M-MLV Reverse Transcriptase (Invitrogen). Gene expression levels were determined by real-time PCR using iTaq Universal SYBR Green Supermix (Biorad) and Biorad CFX96 Real-Time PCR Detection Systems. Relative gene expression was normalized to act-1(T04C12.6) mRNA levels (Chun et al., 2015). In each experiment at least three biological samples were analyzed. The primer sequences used in the quantitative PCR are shown in Table S2.

Feed serotonin (5-HT)

5-HT hydrochloride powder (Sigma) was dissolved in water to a concentration of 0.1M as a stock concentration. Plates were seeded with *E. coli* strain OP50 and 100uL drug was added at a final concentration of 50 mM. Plates were allowed to equilibrate overnight and used the next day (Berendzen et al., 2016).

Lifespan Analysis

Lifespan experiments were performed on NGM plates at 20°C as previously described (Dillin et al., 2002). To prevent progeny production, which resulted in unnatural death of the EGL-20 overexpressed strains, 100uL 10mg/mL 5-fluoro-2'-deoxyuridine (FUdR) was added to seeded plates. Worms were synchronized by egg bleach and were grown on OP50 from hatch, and transit to FUdR plates from L4 to early adulthood. Worms were treated a second time at day 5 of adulthood. Worms were scored every second day. Prism6 software was used for statistical analysis. Log-rank (Mantel-Cox) method was used to determine the significance difference.

QUANTIFICATION AND STATISTICAL ANALYSIS

Statistical parameters, including the exact value of n and descriptive statistics (mean \pm SEM) and statistical significance are reported in the Figures and the Figure Legends. Data are judged to be statistically significant when $p < 0.05$ by two-tailed Student's t test. In figures, asterisks denote statistical significance as calculated by Student's t test (*, $p < 0.05$, **, $p < 0.001$, ***, $p < 0.0001$) as compared to appropriate controls. Lifespans were analyzed using PRISM6 software to determine median survival.

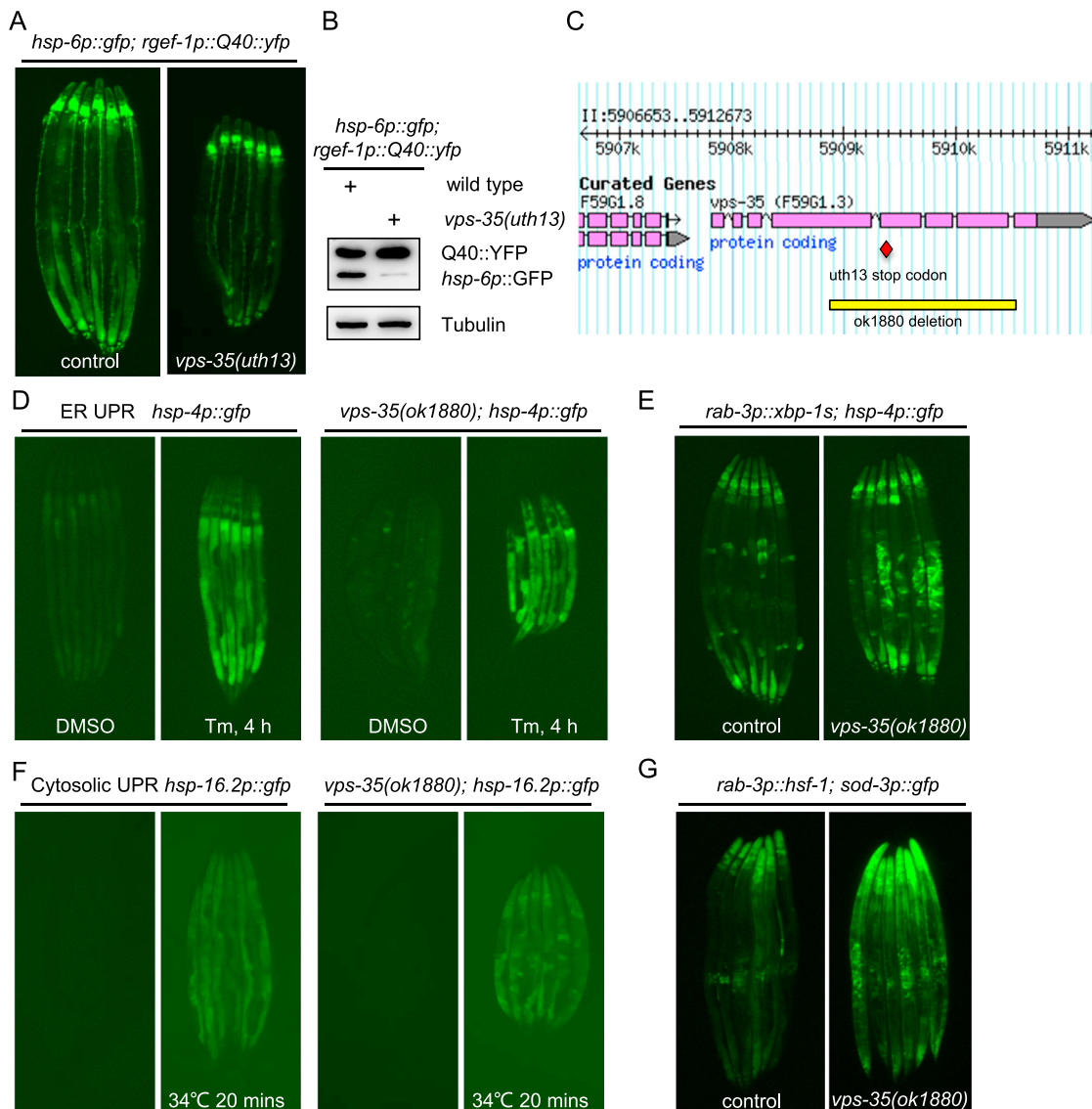


Figure S1. *vps-35(uth13)* Is Required for the Induction of Cell-Non-autonomous UPR^{mt} in Animals Expressing Q40 in Neurons, Related to Figure 1

(A) Representative photomicrographs of *vps-35(uth13)* suppressed *hsp-6p::gfp* induction in the animals expressing Q40::YFP in neurons.

(B) Immunoblots of GFP expression in neuronal Q40::YFP; *hsp-6p::gfp* animals in the presence or absence of *vps-35(uth13)*. Anti-tubulin serves as a loading control.

(C) A schematic of the two mutant alleles *uth13* and *ok1880* of *vps-35* in *C. elegans*.

(D) *vps-35(ok1880)* was not required for the induction of UPR^{ER} reporter *hsp-4p::gfp* when animals were treated with tunicamycin. Synchronized L4 animals were treated with 25ng/ μ l tunicamycin (Tm) or DMSO and rotated in an incubator at 20°C for 4h prior to imaging.

(E) Representative photomicrographs of *vps-35(ok1880)* which had no influence on UPR^{ER} reporter *hsp-4p::gfp* induction in animals expressing spliced XBP-1 in neurons.

(F) *vps-35(ok1880)* is not required for the induction of the cytosolic heat shock stress response reporter *hsp-16.2p::gfp*. Synchronized Day 1 adult animals were placed at 34°C for 20min and allowed to recover for 6h prior to imaging.

(G) Representative photomicrographs of *vps-35(ok1880)* which had no influence on UPR^{cyt} reporter *sod-3p::gfp* in animals expressing HSF-1 in neurons.

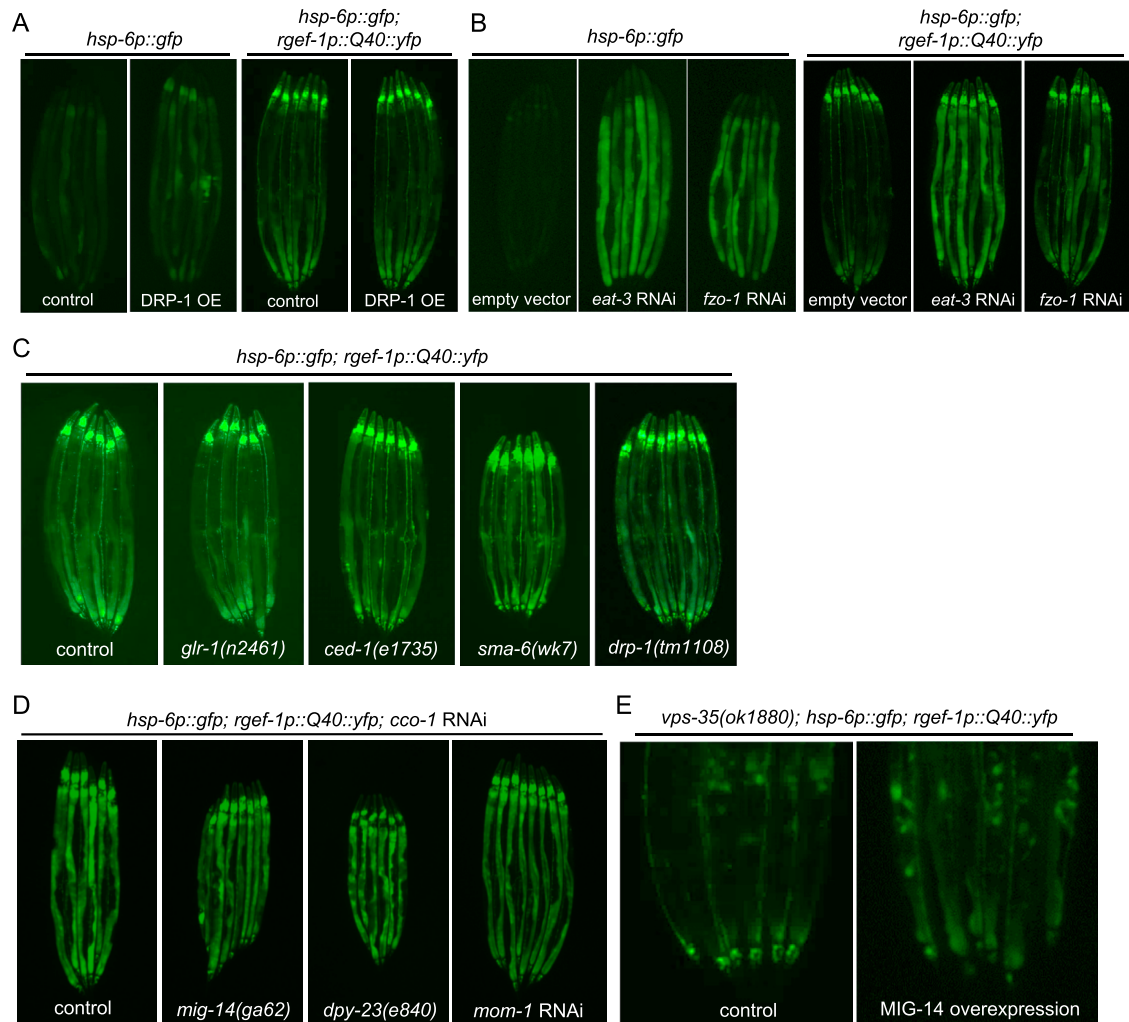


Figure S2. Other Cargo Proteins Retrieved by the Retromer Complex Are Not Required for the Induction of Cell-Non-autonomous UPR^{mt}, Related to Figure 2

(A) Representative photomicrographs of Day 2 adult animals overexpressing DRP-1 in neuronal Q40::YFP; *hsp-6p::gfp* background.

(B) Representative photomicrographs of animals expressing neuronal Q40::YFP; *hsp-6p::gfp* grown on empty vector, *eat-3*, or *fzo-1* RNAi background from hatching.

(C) Representative photomicrographs of Day 2 adult animals expressing neuronal Q40::YFP; *hsp-6p::GFP* in WT, *glr-1(n2461)*, *ced-1(e1735)*, *sma-6(wk7)*, and *drp-1(tm1108)* animals.

(D) Representative photomicrographs of animals expressing neuronal Q40::YFP; *hsp-6p::gfp* in WT, *mig-14(ga62)*, *dpy-23(e840)*, or *mom-1* RNAi background grown on *cco-1* RNAi from hatching.

(E) Representative photomicrographs of overexpressing MIG-14 in *vps-35(ok1880)*; *hsp-6p::gfp*; *rgef-1p::Q40::yfp* background animals. The posterior region of the intestine where *hsp-6p::gfp* is suppressed or induced is shown.

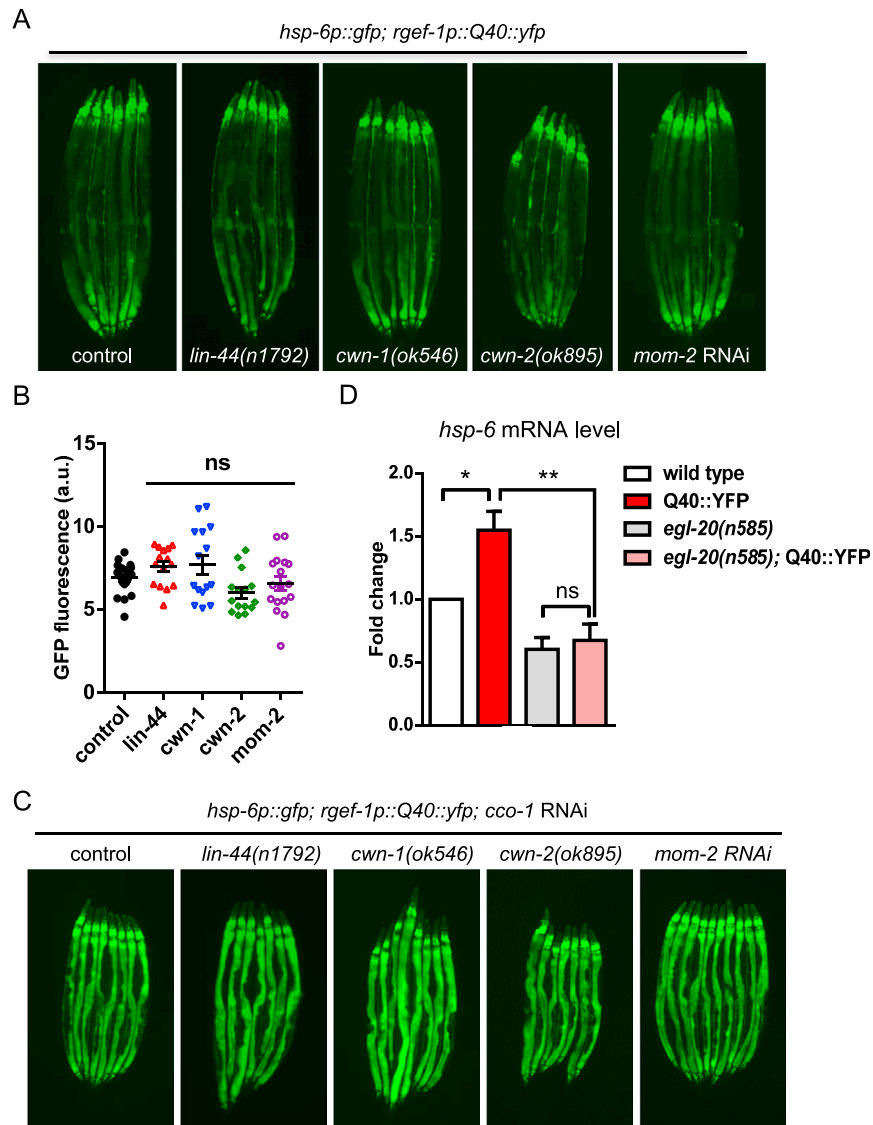


Figure S3. Other Wnt Ligands Are Not Required for the Induction of Cell-Non-autonomous UPR^{mt} in Animals Expressing Q40 in Neurons, Related to Figure 3

(A) Representative photomicrographs of animals expressing neuronal Q40::YFP; *hsp-6p::gfp* in WT, *lin-44(n1792)*, *cwn-1(ok546)*, *cwn-2(ok895)*, or *mom-2* RNAi background.

(B) Quantification of *hsp-6p::gfp* expression in neuronal Q40::YFP animals in the WT, *lin-44(n1792)*, *cwn-1(ok546)*, or *cwn-2(ok895)* background as shown in (A). (***) denotes $p < 0.0001$ via t test. Error bars indicate SEM, $n \geq 20$ worms.)

(C) Representative photomicrographs of animals expressing neuronal Q40::YFP; *hsp-6p::GFP* in WT, *lin-44(n1792)*, *cwn-1(ok546)*, *cwn-2(ok895)*, or *mom-2* RNAi background grown on *cco-1* RNAi from hatching.

(D) Quantitative PCR of *hsp-6* mRNA level. Synchronized Day 1 adult animals of WT, *rgef-1p::Q40::yfp*, *egl-20(n585)*, or *rgef-1p::Q40::yfp;egl-20(n585)* were collected for qPCR. * $p < 0.05$, ** $p < 0.01$ via t test. Error bars indicate the SEM from four biological replicates.

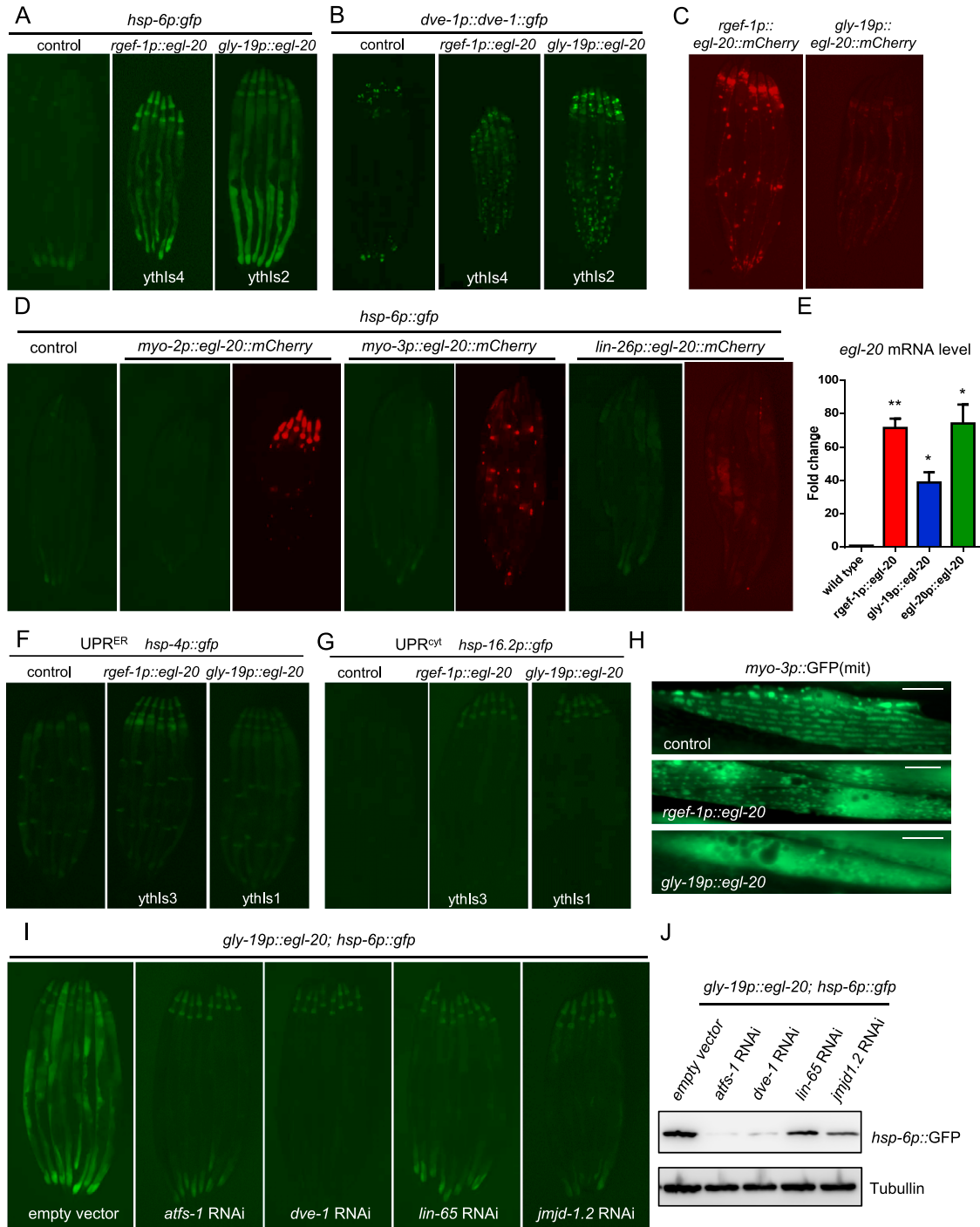


Figure S4. Expression of Wnt Ligand/EGL-20 Had a Specific Effect on UPR^{mt}, Related to Figure 4

(A) Representative photomicrographs of *hsp-6p::gfp* reporter animals in WT and two additional *egl-20* transgenic animals. Strains used in this figure are yths4 [*rgef-1p::egl-20; myo-2p::tdTomato*] and yths2 [*gly-19p::egl-20; myo-2p::tdTomato*].

(B) Representative photomicrographs of DVE-1::GFP reporter animals in WT, yths4 [*rgef-1p::egl-20; myo-2p::tdTomato*], or yths2 [*gly-19p::egl-20; myo-2p::tdTomato*] background.

(C) Representative photomicrographs of *rgef-1p::egl-20::mCherry* animals and *gly-19p::egl-20::mCherry* animals in a WT background. Images were taken at Day 1 of adulthood. EGL-20 was specifically expressed in the neurons with *rgef-1* promoter and expressed in the intestine with *gly-19* promoter.

(D) Representative photomicrographs of *hsp-6p::gfp* reporter animals in WT, ythEx43 [*myo-2p::egl-20::mCherry*], ythEx39 [*myo-3p::egl-20::mCherry*] or ythEx44 [*lin-26p::egl-20::mCherry*] background. EGL-20 expression in the pharynx (*myo-2* promoter), in the muscle cells (*myo-3* promoter), or in the hypodermal cells (*lin-26* promoter) are not able to induce the expression of the *hsp-6p::gfp* reporter.

(legend continued on next page)

-
- (E) Transcript levels of *egl-20* in animals expressing *egl-20* in neurons (*ythls3[rgef-1p::egl-20; myo-2p::tdTomato]*), in the intestine (*ythls1[gly-19p::egl-20; myo-2p::tdTomato]*), or in the Wnt-producing cells (*ythls8[egl-20p::egl-20::mCherry; pRF6(rol-6)]*) at Day 1 of adulthood were measured by QPCR. Results are shown relative to transcript levels in WT animals with error bars indicate SEM from three biological replicates. (** denotes $p < 0.01$, * denotes $p < 0.05$ via-t test)
- (F) Representative photomicrographs of *hsp-4p::gfp* UPR^{ER} reporter animals in WT, *ythls3[rgef-1p::egl-20; myo-2p::tdTomato]*, and *ythls1[gly-19p::egl-20; myo-2p::tdTomato]* background.
- (G) Representative photomicrographs of *hsp-16.2p::gfp* UPR^{CVI} reporter animals in WT, *ythls3[rgef-1p::egl-20; myo-2p::tdTomato]*, and *ythls1[gly-19p::egl-20; myo-2p::tdTomato]* background.
- (H) Representative photomicrographs of the mitochondrial morphology of muscle cells in WT, *ythls3[rgef-1p::egl-20; myo-2p::tdTomato]*, and *ythls1[gly-19p::egl-20; myo-2p::tdTomato]* background, which was marked by *myo-3p::GFP(mit)*. Scale bar represents 10 μm .
- (I) Representative photomicrographs of *ythls3[gly-19p::egl-20; myo-2p::tdTomato]*; *hsp-6p::gfp* reporter animals grown on EV, *atfs-1* RNAi, *dve-1* RNAi, *lin-65* RNAi, or *jmjd-1.2* RNAi from hatching. Images were taken of Day 1 adult animals.
- (J) Immunoblot of *hsp-6p::GFP* expression in animals grown on EV, *atfs-1* RNAi, *dve-1* RNAi, *lin-65* RNAi, or *jmjd-1.2* RNAi from hatching.

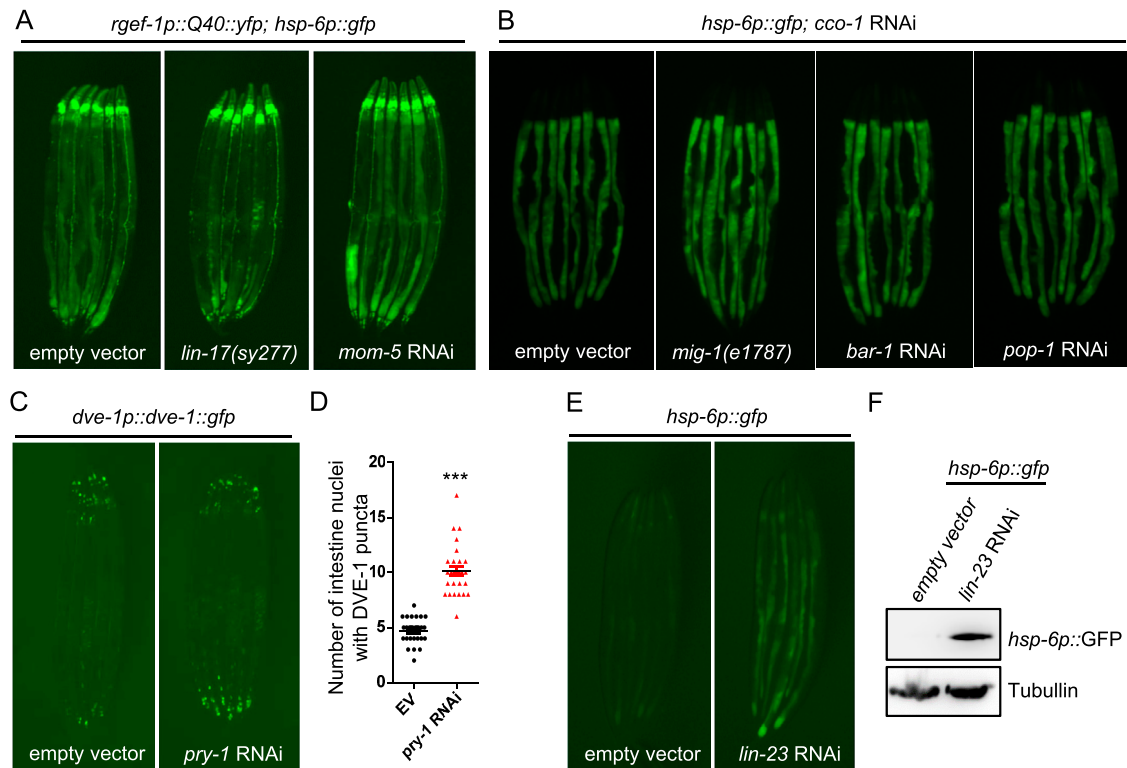


Figure S5. Other Wnt Receptors Are Not Required for the Induction of Cell-Non-autonomous UPR^{mt} in Animals Expressing Q40::YFP in Neurons, Related to Figure 5

(A) Representative photomicrographs of neuronal Q40::YFP; *hsp-6p::gfp* animals in WT, *lin-17(sy277)*, or *mom-5* RNAi background.

(B) Representative photomicrographs of *hsp-6p::gfp* animals in WT, *mig-1(e1787)*, *bar-1* RNAi, or *pop-1* RNAi background grown on *cco-1* RNAi from hatching as indicated. *hsp-6p::gfp* expression was not affected in *mig-1(e1787)*, *bar-1* RNAi, and *pop-1* RNAi animals.

(C) Representative photomicrographs of animals expressing DVE-1::GFP reporter grown on EV or *pry-1* RNAi from hatching as indicated. DVE-1::GFP is accumulated in the *pry-1* RNAi animals.

(D) Quantification of the number of intestinal nuclei with DVE-1 expression. The genotypes are as in (C). (***) denotes $p < 0.0001$ via t test. Error bars indicate SEM, $n \geq 30$ worms).

(E) Representative photomicrographs of animals expressing *hsp-6p::GFP* grown on EV or *lin-23* RNAi from hatching. *hsp-6p::GFP* expression was induced in *lin-23* RNAi animals.

(F) Immunoblot of GFP expression in *hsp-6p::gfp* animals grown on EV or *lin-23* RNAi from hatching. The genotypes are as in (E). Anti-tubulin serves as a loading control.

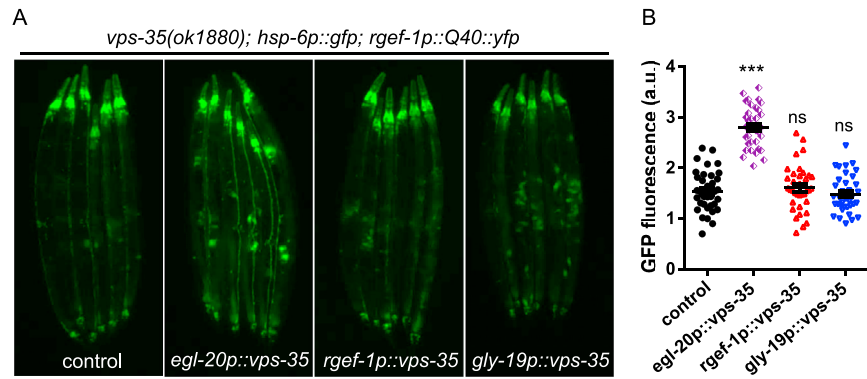


Figure S6. Expression of *vps-35* in Wnt/EGL-20 Producing Cells Strongly Rescued the Suppression of the *hsp-6p::gfp* Reporter in the *vps-35* Mutants with Neuronal Q40 Expression, Related to Figure 6

(A) Representative photomicrographs of *vps-35(ok1880)*; neuronal Q40::YFP; *hsp-6p::gfp* animals with or without *egl-20p::vps-35*, *rgef-1p::vps-35*, *gly-19p::vps-35* rescue as indicated.

(B) Quantification of *hsp-6p::gfp* expression in *vps-35(ok1880)*; neuronal Q40::YFP; *hsp-6p::gfp* animals with or without *egl-20p::vps-35*, *rgef-1p::vps-35*, *gly-19p::vps-35* rescue. The genotypes are as in (A). (***) denotes $p < 0.0001$ via t test, ns denotes $p > 0.05$ via t test. Error bars indicate SEM, $n \geq 30$ worms)

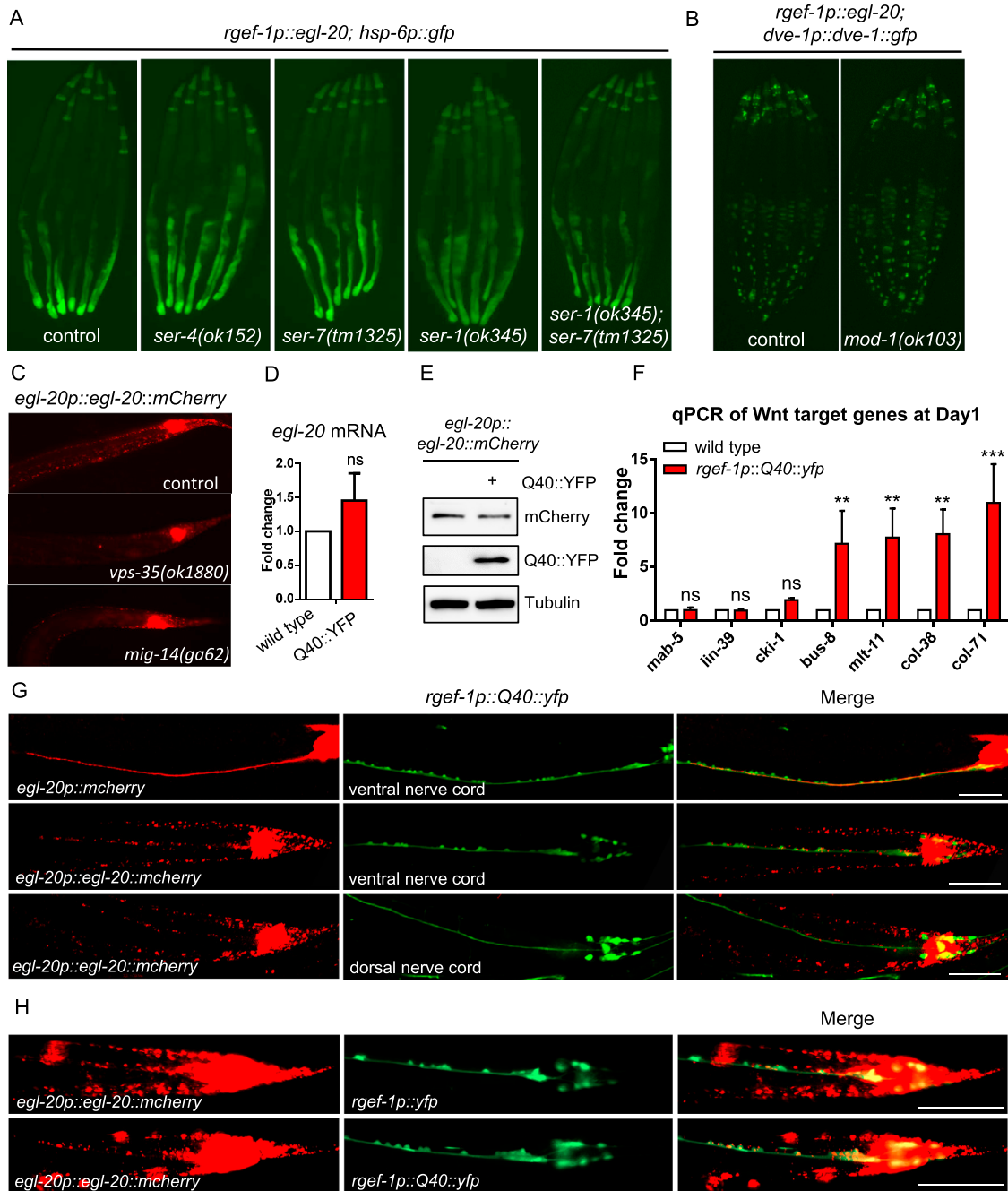


Figure S7. EGL-20 Is Expressed in Neurons in *C. elegans*, Related to Figure 7

(A) Representative photomicrographs of animals expressing neuronal EGL-20; *hsp-6p::gfp* in WT, *ser-4(ok152)*, *ser-7(tm1325)*, *ser-1(ok345)*, or *ser-1(ok345); ser-7(tm1325)* double mutants background.

(B) Representative photomicrographs of animals expressing neuronal EGL-20; *dve-1p::dve-1::gfp* in WT or *mod-1(ok103)* background.

(C) Representative photomicrographs of *egl-20p::egl-20::mCherry* in WT, *vps-35(ok1880)*, or *mig-14(ga62)* background.

(D) Quantitative PCR of *egl-20* mRNA level. Synchronized Day 1 adult animals of WT, *rgef-1p::Q40::yfp* were collected for qPCR. ns denotes $p > 0.05$ via t test. Error bar indicates the SEM from six biological replicates.

(E) Immunoblots of mCherry and YFP expression in *egl-20p::egl-20::mCherry* animals in the presence or absence of neuronal Q40. Anti-tubulin serves as a loading control.

(F) Quantitative PCR of Wnt target genes mRNA level. Synchronized Day 1 adult animals of WT and *rgef-1p::Q40::yfp* were collected for qPCR. * $p < 0.05$, ** $p < 0.01$, ns denotes $p > 0.05$ via t test. Error bars indicates the SEM from six biological replicates.

(legend continued on next page)

(G) Representative of three center images of confocal photomicrographs of animals expressing *egl-20p::mcherry* or *egl-20p::egl-20p::mCherry* in combination with *rgef-1p::Q40::yfp*. Scale bar represents 50 μm .

(H) Representative photomicrographs of animals expressing *egl-20p::egl-20p::mCherry* in combination with *rgef-1p::yfp* or *rgef-1p::Q40::yfp*. Scale bar represents 50 μm .